Leveraging Computational Fluid Dynamics (CFD) for Complex MEP System Design Challenges: A Comprehensive Exploration through Real-World Case Studies

By

Dung Vu, Ph.D., PE, QCxP, LEED AP

MEP Green Design and Build, PLLC

Abstract

The design of Mechanical, Electrical, and Plumbing (MEP) systems for buildings stands as a crucial element in contemporary building design, where the optimization of MEP systems performance presents challenges, particularly in the context of complex facilities. Computational Fluid Dynamics (CFD) has appeared as an important tool to address these challenges. In this article, we delve deep into the application of CFD, employing technical language, through real-world case studies. Each case study explains how CFD effectively resolves complex MEP design challenges, providing invaluable insights for MEP engineers and designers.

Introduction

Mechanical, Electrical, and Plumbing (MEP) systems are essential components of building infrastructure, tasked with ensuring peak performance, efficiency, safety, code/standard compliance and occupant comfort. For MEP engineers, designing the most efficient MEP systems that fulfill demanding criteria in various building operation environments, meet project owner requirements, and comply with relevant codes, all in a cost-effective and sustainable manner, has always been a persistent and formidable challenge.

Complexities further escalate when dealing with factors that are challenging to control during the design stage, especially in scenarios where buildings exhibit substantial dimensions, towering ceiling heights, or vast footprints, as seen in hypermarkets, sports stadiums, and similar facilities. Additionally, spaces with stringent requirements for precise temperature and humidity control, such as hospital operating rooms, data centers, cleanrooms, laboratories, and pharmaceutical facilities, introduce an additional layer of complexity.

The challenges mentioned above are further intensified when traditional design methodologies prove unreliable in guaranteeing the accurate translation of intended system performance into the realities of real-world building operations. Moreover, conventional MEP design approaches face challenges in offering comprehensive insights into various design alternatives and "What if" operational scenarios. They often struggle with making well-informed decisions to identify the optimal choice among various MEP system options, a challenge that becomes particularly pronounced when cost-effectiveness is a crucial determinant in selecting the preferred alternatives.

Given the multifaceted challenges inherent in MEP system design, it has become imperative to leverage advanced tools and methodologies to achieve superior MEP systems designs. This involves addressing issues related to "what if" operational scenarios, validating the MEP design, ultimately ensuring the accuracy and efficacy of the MEP design process.

One of the powerful tools that has emerged to handle these complex MEP design challenges, particularly those associated with mechanical and plumbing systems, is Computational Fluid Dynamics (CFD). CFD refers to the application of numerical methods and computer simulations to analyze the patterns of airflows, heat transfer, and fluid dynamics within a building's mechanical and plumbing systems. CFD equips MEP engineers with the capacity to examine and simulate complex MEP system challenges with enhanced precision and efficiency, streamlining the design process.

In this article, we embark on a journey investigating into a series of comprehensive CFD-driven real-world case studies, each representing typical challenges encountered in MEP design. The initial case

involves utilizing CFD to examine and offer suggestions and recommendations for the existing MEP design of a data center. The subsequent study employs CFD to validate the design of the ventilation system within the operation room of a hospital. The final case focuses on using CFD to determine the optimal solution, addressing the "what if" scenarios for the design of the mechanical system of the basement level of the parking garage.

These case studies are particularly designed to illustrate the efficacy and applicability of CFD in solving the complex MEP design challenges that have long confounded engineers and designers. Each case study will provide a profound exploration of the intricate details of MEP systems, showcasing how CFD simulations offer engineers and designers the powerful tools required to achieve optimization and innovation within this crucial domain.

Case Study 1

Utilizing CFD Simulation Analysis to verify the HVAC system design for Data Center

San Juan, Puerto Rico

Data centers serve as the backbone of the digital age, housing an ever-expanding expanse of servers and computational infrastructure. The seamless operation of these data centers relies heavily on precise control of temperature, humidity and air distribution to safeguard against server overheating and minimize the risk of downtime.

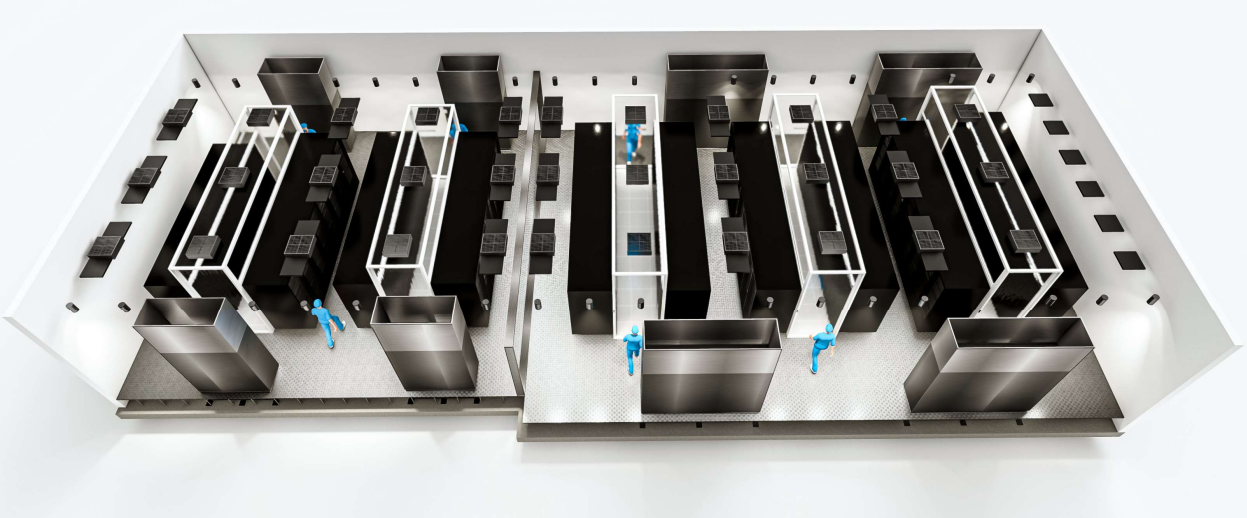

In our first case study, we apply CFD model analysis to verify the HVAC system design for a new 3,263 square feet Data Center/SCADA Room with 18 inches raised floor in a facility in San Juan, Puerto Rico. The primary objective of this CFD simulation is to examine the distribution of temperature, humidity, static pressure, and air velocity in the hot-aisle server/Scada containment for Day 1 and Day 2 rack configuration loads, specifically for n+1 configurations. Please refer to the images below for a floor plan of the Data Center/Scada room with the location of the racks and CRAC units, along with a breakdown of racks for Day 1 and Day 2 configurations and its loads as follows:

Day One Partial Build out: 54 Racks Total Configuration (235kW):

SCADA / EMS - Total Load (75kW):

- 10 - Server Racks (5.5kW)
- 7 – Network Racks (2.5kW)
- 1 – LMR Racks (2.5kW)

DATA CENTER AREA - Total Load (160kW):

- 24 - Server Racks (5.5kW)
- 8 – Network Racks (2.5kW)
- 4 – Other Racks (2.0kW)

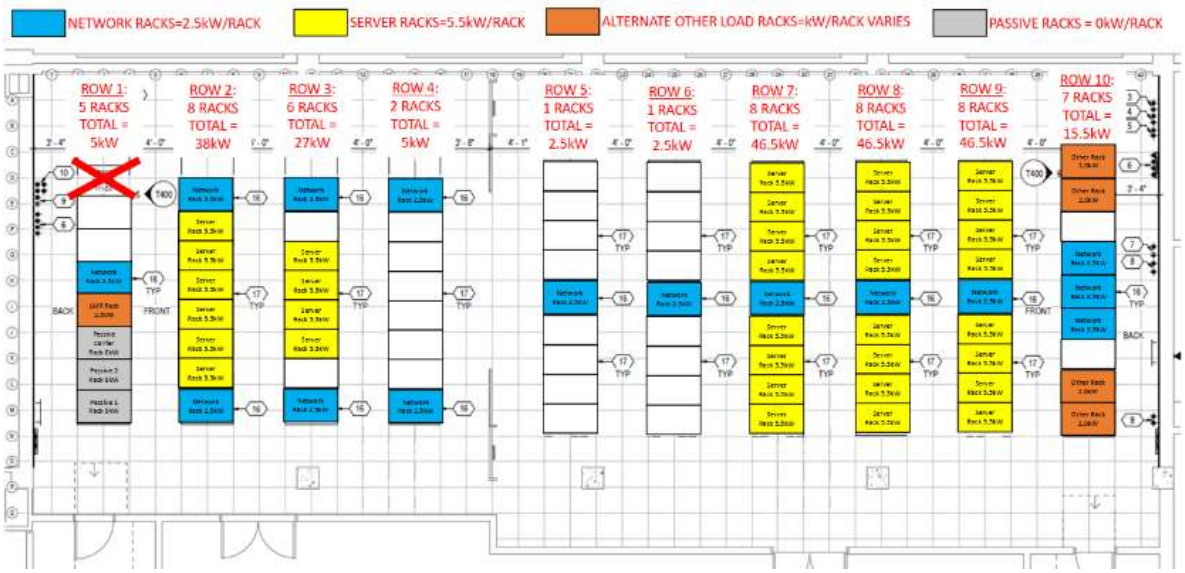

Day Two Full Buildout: 85 Racks Total Configuration (383kW):

SCADA / EMS - Total Load (124kW):

- 18 - Server Racks (5.5kW)
- 7 – Network Racks (2.5kW)
- 1 – LMR Racks (2.5kW)
- 1 – Carrier Rack (2.5kW)
- 1 – Future Rack (2.5kW)
- 3 – Passive Racks (0kW)

DATA CENTER AREA - Total Load (259kW):

- 42- Server Racks (5.5kW)
- 8 – Network Racks (2.5kW)
- 4 – Other Racks (2.0kW)

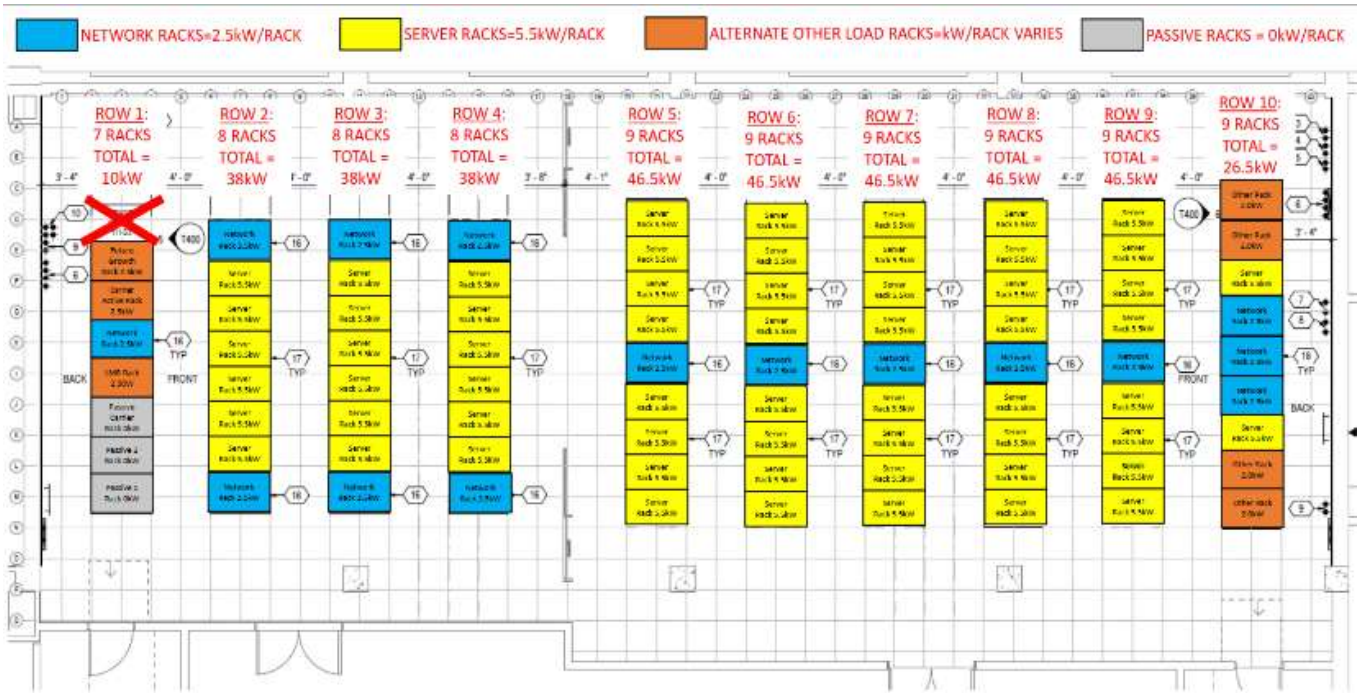

The following are being taken into consideration for the Data Center HVAC design:

The system consists of N+1 capacity Computer Room Air Conditioner (CRAC) units, " cold aisle/hot aisle" air distribution design (which consists of air supply aisles at the front of the racks with a containment system to enhance the cooling system's performance and a ceiling return plenum up through the aisle at the rear of the racks.) CRAC units shall consist of a supply fan, chilled water-cooling coil, dehumidification control, MERV 13 filter, and access sections.

Ambient temperatures inside the equipment room shall be maintained within the specified range tailored to the requirements of each equipment. The designed HVAC system shall be capable of maintaining interior conditions of 64°F to 81°F (17.8°C to 27°C) and reduce humidity to a level of 30% to 60% relative humidity (RH) with a dew point range of 42 °F to 59 °F (5.5 °C to 15 °C) per ANSI/TIA 569. In addition, the most crucial factor for maintaining optimal functionality and preventing overheating in both the Data and SCADA rooms is to verify the inlet and exit temperatures of the IT racks. According to ASHRAE 2021 standards for Class-I servers, the recommended temperature range is 64.4 to 80.6 °F, with the allowable range being slightly broader, spanning from 59 to 89.6 °F. Our assessment of the HVAC system's effectiveness for this data center will be based on adhering to these critical temperature thresholds, determining whether it passes or fails.

The sensible heat loads due to the occupants and the ceiling lights were assumed to be 1500 Btu/h (440 W) and 2457 Btu/h (720 W), respectively. The total sensible heat load due to the other equipment, including 8 numbers of CRAC was assumed to be 3583 Btu/h (1050 W). It's important to note that HVAC systems are not specifically designed for the data room itself; instead, they are focused on cooling the data racks within the hot aisle. The Data Center HVAC System shall be designed to be concurrently maintainable in accordance with the Uptime Institute Tier III reliability category.

Results and Discussion

Temperature Distribution

With the current HVAC design, which includes Computer Room Air Conditioning (CRAC) units with an External Static Pressure (ESP) of 0.2 W.G and a Leaving Air Temperature (LAT) of 55 °F.

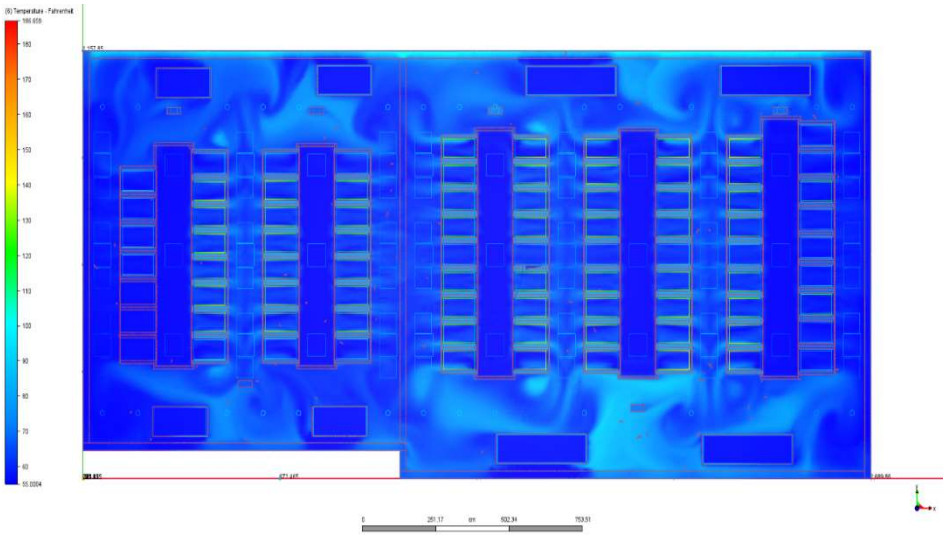

Figure 1.1

The temperature distribution in the data center at 1 foot above ground level **(ESP=0.2 IN WG, LAT=55°F)**

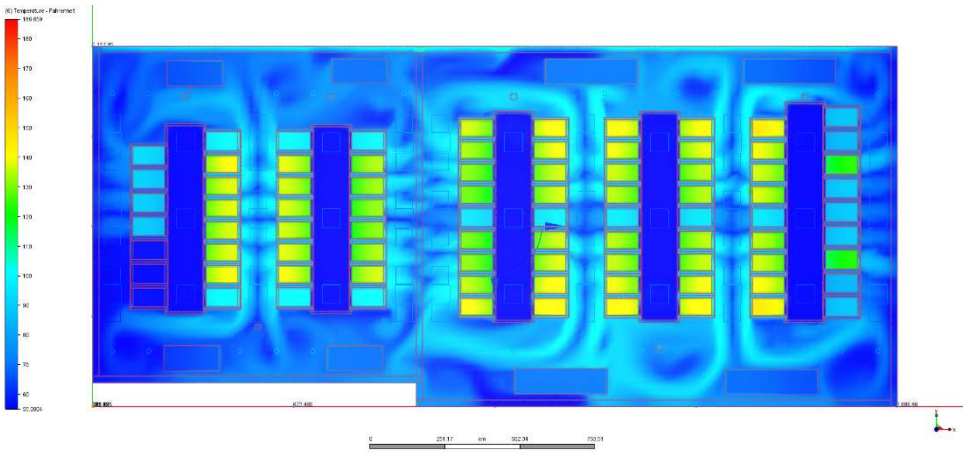

Figure 1.2

The temperature distribution in the data center at 5 feet above ground level **(ESP=0.2 IN WG, LAT=55°F)**

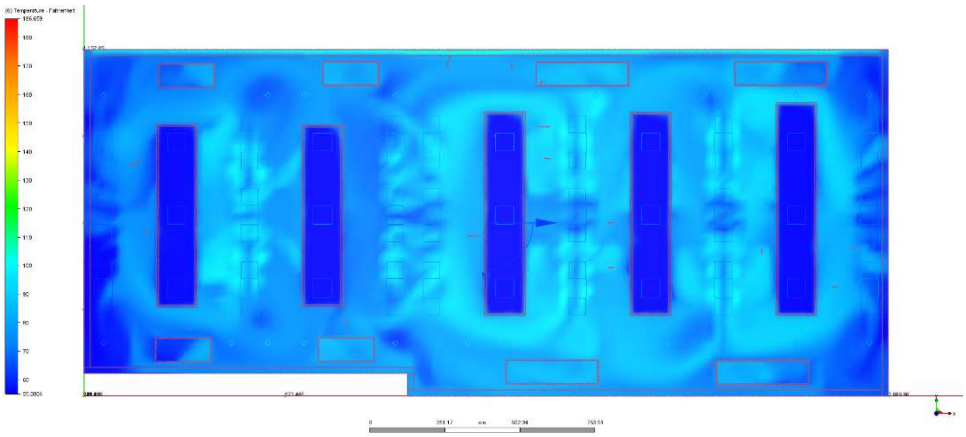

Figure 1.3

The temperature distribution in the data center at 9 feet above ground level **(ESP=0.2 IN WG, LAT=55°F)**

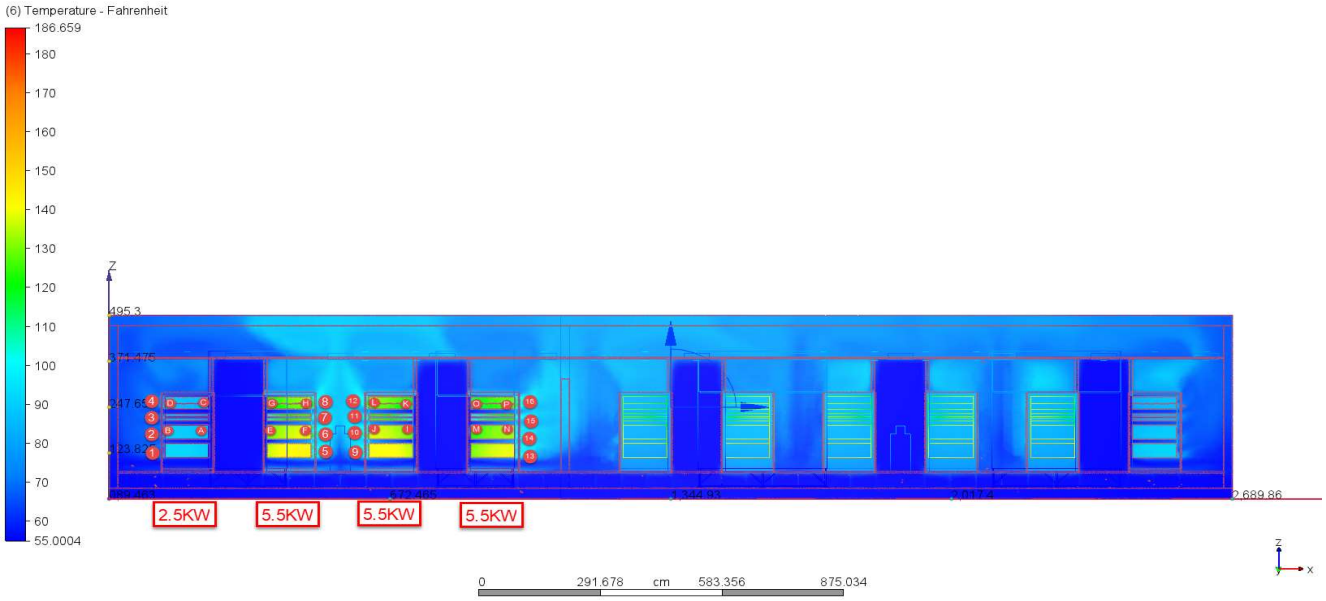

Figure 2.1 Sectional view and temperature chart vertically across the server racks - Scada Room.

(ESP=0.2 IN WG, LAT=55°F)

The temperature analysis chart for the racks' entering air temperature in Scada room **(ESP=0.2 IN WG, LAT=55°F)**

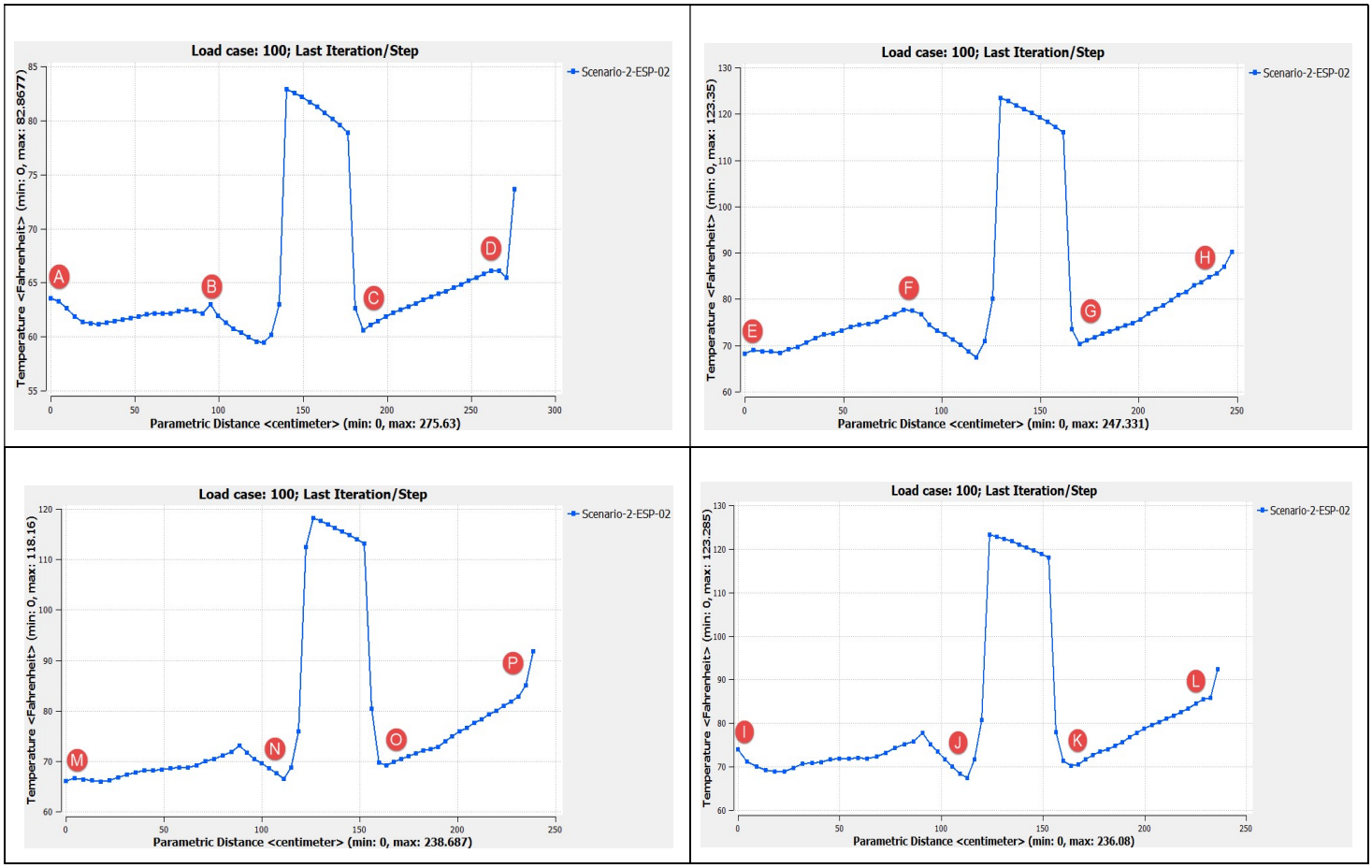

The temperature analysis chart for the rack's leaving air temperature in Scada room **(ESP=0.2 IN WG, LAT=55°F)**

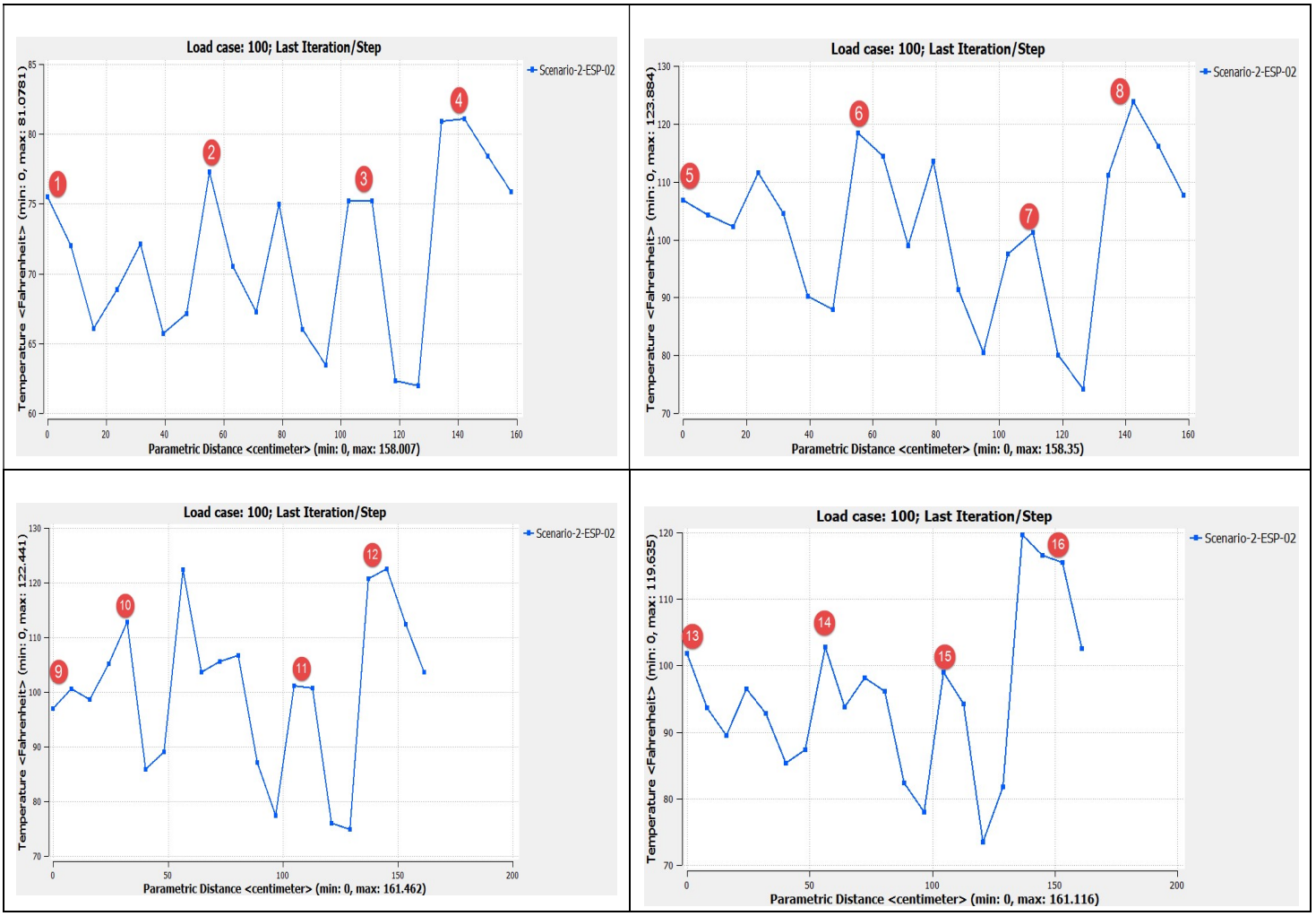

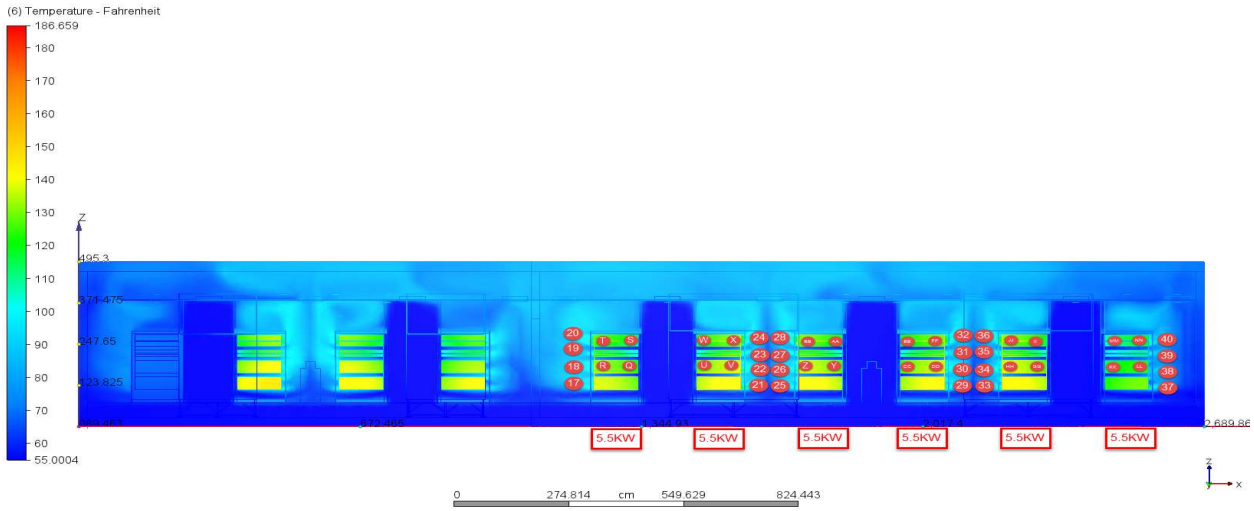

Figure 2.2 Sectional view and temperature chart vertically across the server racks – Data Center

The temperature analysis chart for the racks' entering air temperature in Data Center Room **(ESP=0.2 IN WG, LAT=55°F)**

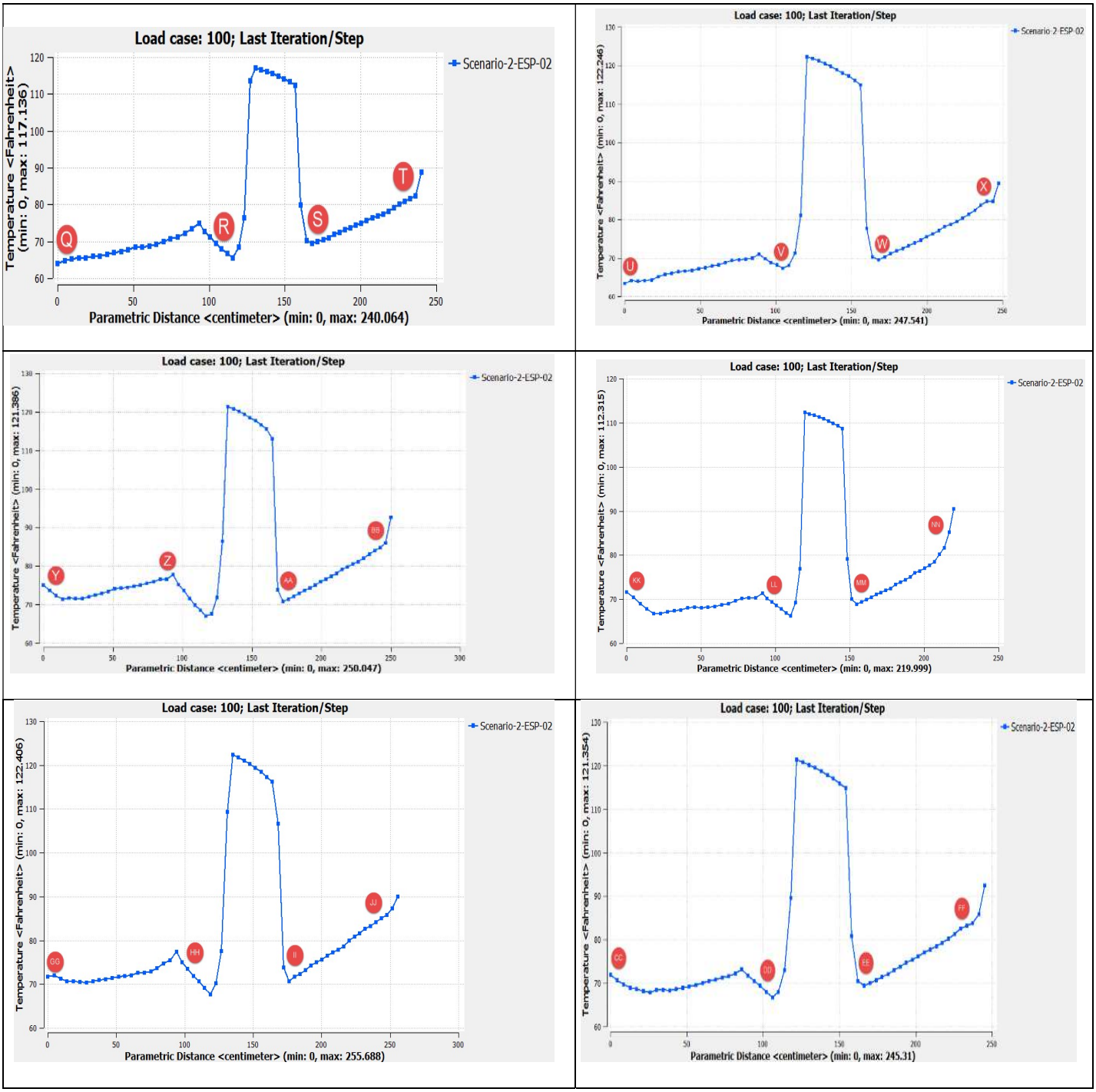

The temperature analysis chart for the rack's leaving air temperature in Data Center room **(ESP=0.2 IN WG, LAT=55°F)**

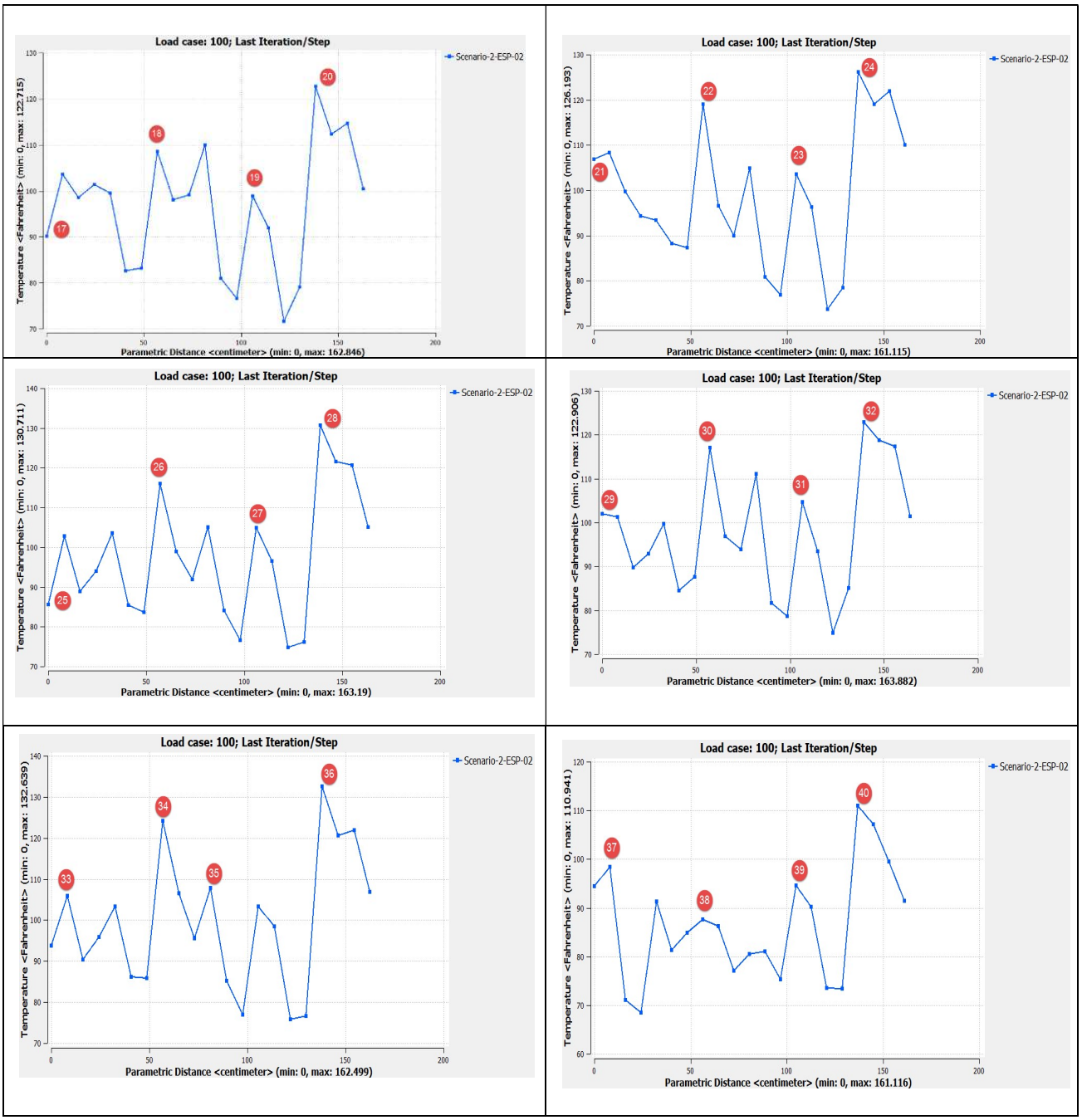

Figures 1.1, 1.2 and 1.3 illustrates temperature variations at heights of 1', 5', and 9' above the floor. Cold air supplied by the CRAC units pass through the raised floors and perforated grilles, entering the cold aisle. From there, it is directed into the server inlets. The heated air exits the server racks through the rear, entering the hot aisle. Subsequently, this air combines with the room's return air before circulating back to the CRAC units. The return path involves passing through the ceiling return plenum of the data center.

This airflow pattern explains the temperature distribution at elevations of 1', 5', and 9' above ground level. At the 1' level, the air temperature closely approximates the leaving air temperature of the CRAC units (55 °F). Similarly, the air temperature at the 9' level closely corresponds to the room's return air temperature. Particularly, the most significant temperature rise occurs at the 5' level, the midplane level, where direct heat exchange takes place between the hot and cold air within the mid-plane of the data room. This phenomenon is clearly illustrated in the section view accompanying the temperature chart, as depicted in **Figure 2.1 and 2.2**

The thermal map depicted in **Figure 2.1 and 2.2** reveals the exit temperature from the racks in the Scada and Data room exceeds the permissible limits outlined in the **Table 2.1 of ASHRAE 2021** guidelines - 15 to 32°C (59 to 90 °F)

Table 2.1 2021 Thermal Guidelines for Air Cooling— SI Version (I-P Version in Appendix B)

Equipment Environment Specifications for Air Cooling							
	Product Operation[b,c]					Product Power Off[c,d]	
Class[a]	Dry-Bulb Temp.[e,g], °C	Humidity Range, Noncond.[h, i, k, l, n]	Max. Dew Point[k], °C	Max. Elev.[e,j,m], m	Max. Rate of Change[f], °C/h	Dry-Bulb Temp., °C	RH[k], %
Recommended (suitable for Classes A1 to A4; explore data center metrics in this book for conditions outside this range.)							
A1 to A4	18 to 27	–9°C DP to 15°C DP and 70% rh[n] or 50% rh[n]					
Allowable							
A1	15 to 32	–12°C DP and 8% rh to 17°C DP and 80% rh[k]	17	3050	5/20	5 to 45	8 to 80[k]
A2	10 to 35	–12°C DP and 8% rh to 21°C DP and 80% rh[k]	21	3050	5/20	5 to 45	8 to 80[k]
A3	5 to 40	–12°C DP and 8% rh to 24°C DP and 85% rh[k]	24	3050	5/20	5 to 45	8 to 80[k]
A4	5 to 45	–12°C DP and 8% rh to 24°C DP and 90% rh[k]	24	3050	5/20	5 to 45	8 to 80[k]

The entering air temperature for the rack in the SCADA Room and Data Center, as indicated below, meets the ASHRAE guidelines.

Entering Air Temperature: ESP-=0.2 in wg @ 55°F - Scada Room								
Rack Type	2.5kw		5.5kw		5.5kw		5.5kw	
Entering points	A	C	E	G	M	O	I	K
EAT Display temperatures (°F)	64	61	70	72	66	68	75	74

Entering Air Temperature: ESP-=0.2 in wg @ 55°F - Data Center Room												
Rack Type	5.5KW		5.5KW		5.5KW		5.5KW		5.5KW		5.5KW	
Entering points	Q	S	U	W	Y	AA	EE	CC	II	GG	MM	KK
EAT Display temperatures (°F)	64	71	64	70	77	71	70	71	70	71	70	72

Leaving Air Temperature Analysis: ESP-=0.2 in wg @ 55°F										
Room	Scada				Data Center					
Tagged Point	1--4	5--8	9--12	13--16	17--20	21--24	25--28	29--32	33--36	37--40
Leaving Air Temperature behind the Rack (°F)	75.51	106.73	96.96	101.82	90.12	106.82	85.57	102.05	93.72	94.47
	72.02	104.28	100.49	93.60	103.62	108.26	102.86	101.27	105.84	98.45
	66.04	102.28	98.61	89.42	98.56	99.67	88.91	89.82	90.32	71.02
	68.84	111.46	105.17	96.48	101.38	94.30	93.95	92.95	95.92	68.52
	72.12	104.50	112.75	92.80	99.46	93.37	103.51	99.67	103.33	91.35
	65.68	90.25	85.87	85.29	82.57	88.17	85.44	84.45	86.16	81.28
	67.10	87.88	89.10	87.34	83.24	87.35	83.62	87.67	85.85	84.87
	77.26	118.45	122.41	102.79	108.57	118.98	115.97	117.08	124.09	87.55
	70.51	114.38	103.57	93.75	98.08	96.54	98.98	96.92	106.61	86.29
	67.22	98.88	105.50	98.12	99.07	89.99	91.88	93.89	95.60	77.03
	74.94	113.47	106.65	96.14	109.92	104.84	105.09	111.02	107.90	80.47
	66.02	91.36	87.06	82.31	80.90	80.77	84.07	81.63	85.17	81.03
	63.47	80.42	77.40	77.96	76.59	76.87	76.54	78.72	76.96	75.31
	75.18	97.54	101.17	98.93	98.91	103.59	104.96	104.66	103.33	94.60
	75.19	101.27	100.76	94.25	91.96	96.28	96.47	93.45	98.49	90.15
	62.33	80.08	75.99	73.48	71.70	73.70	74.76	74.77	75.77	73.58
	61.99	74.15	74.89	81.76	79.12	78.46	76.20	85.05	76.69	73.42
	80.92	111.13	120.73	119.64	122.72	126.19	130.71	122.91	132.64	110.94
	81.08	123.88	122.44	116.55	112.38	118.99	121.64	118.74	120.58	107.19
	78.38	116.04	112.36	115.48	114.72	121.91	120.69	117.35	121.82	99.52
	75.83	107.65	103.66	102.57	100.40	110.08	105.15	101.48	106.82	91.49
Minimum(°F)	61.99	74.15	74.89	73.48	71.70	73.70	74.76	74.77	75.77	68.52
Maximum(°F)	81.08	123.88	122.44	119.64	122.72	126.19	130.71	122.91	132.64	110.94
Average(°F)	71.31	101.72	100.17	95.26	96.38	98.82	97.47	97.88	99.70	86.60

However, instances of leaving air temperature at points corresponding to 5-8, 9-12, 13-16, 17-20, 21-24, 25-28, 29-32, 33-36, and 37-40, as displayed in the table above, exceed 90°F in both the SCADA and Data Center rooms. This surpasses the acceptable specifications for equipment environments.

Recognizing the failure to meet the allowable temperature limits for server racks with the current HVAC design, which is crucial for determining the right specifications of the HVAC system for the data center's design requirements, we have decided to manipulate two key parameters in the CRAC specifications. Firstly, we have adjusted the external static pressure (ESP) to ensure an adequate static pressure reaches the cold aisle. Secondly, we have reduced the leaving air temperature (LAT) of the CRAC units to increase their cooling effectiveness, particularly leveraging the available chilled water system for the data center. This involved a gradual increase in ESP and a reduction in LAT, with the resulting thermal map of the server racks at 5’ level shown in **Figure 4.**

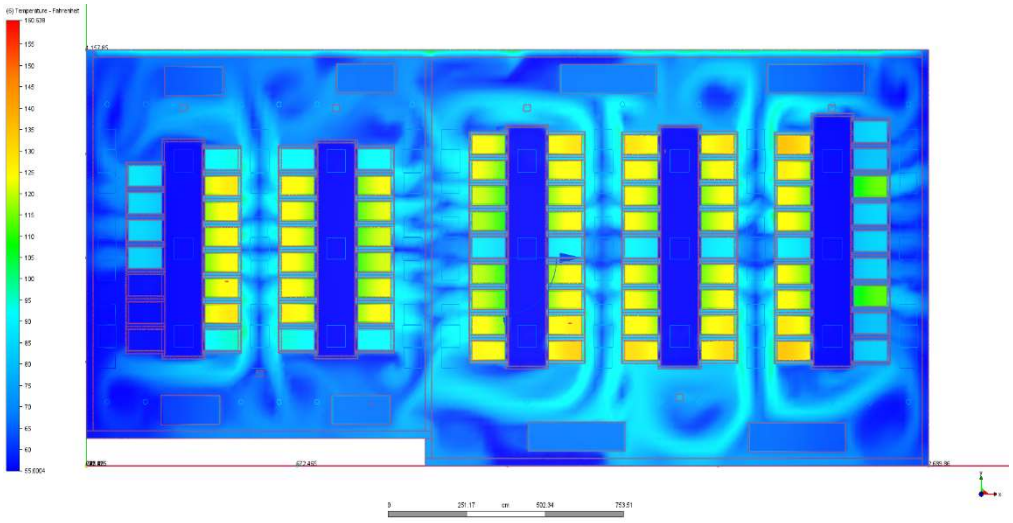

Figure 4.1 The temperature distribution at 5 foot above ground level (ESP=0.3 IN WG, LAT=55°F)

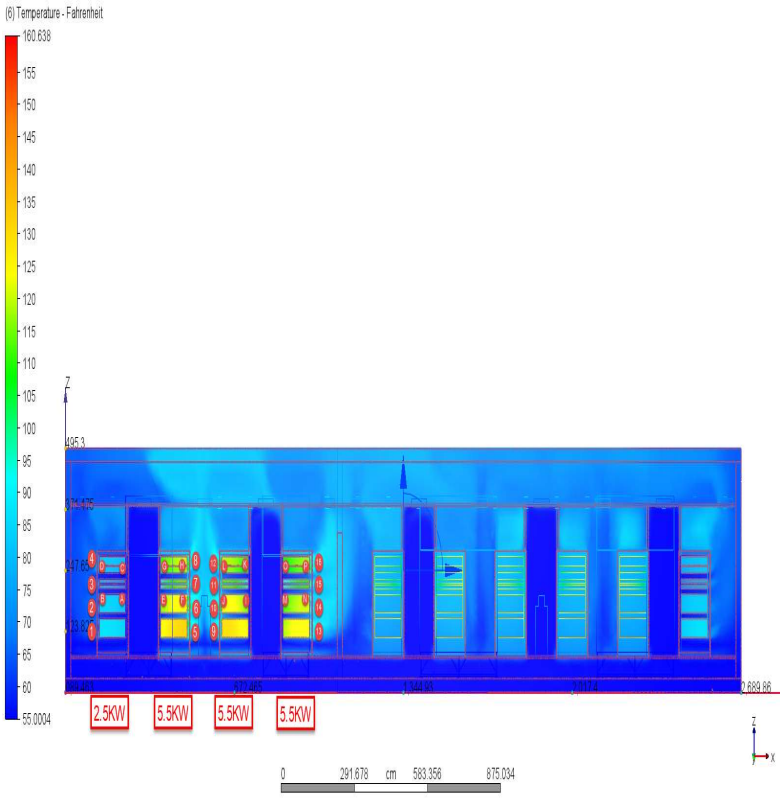

Figure 4.1a
Section View in Scada Room (ESP=0.3 IN WG, LAT=55°F)

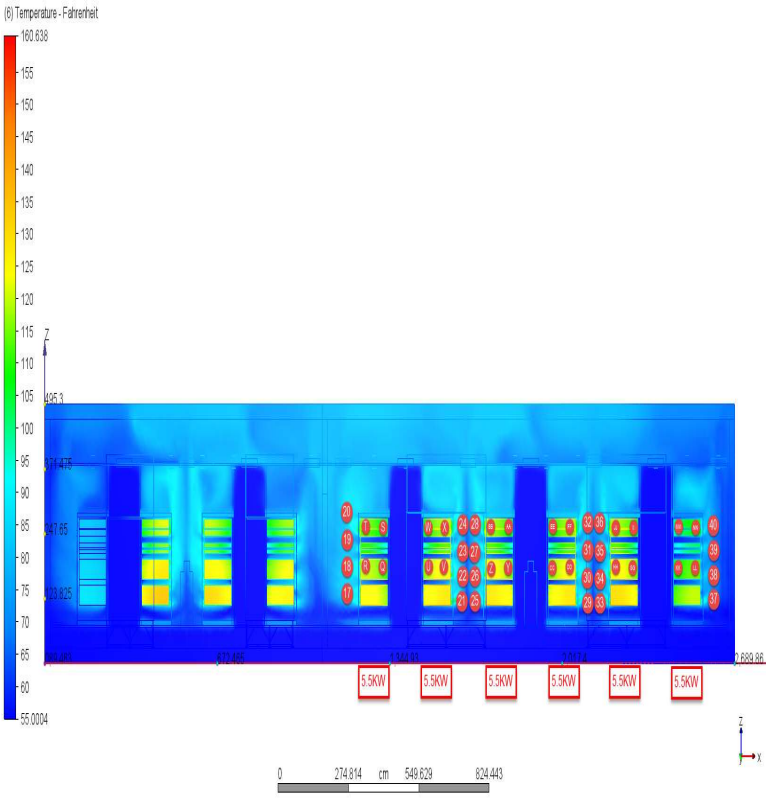

Figure 4.1b
Section View in Data Center Room (ESP=0.3 IN WG, LAT=55°F)

Entering Air Temperature: ESP-=0.3 in wg @ 55°F - Scada Room								
Rack Type	2.5kw		5.5kw		5.5kw		5.5kw	
Entering points	A	C	E	G	M	O	I	K
EAT Display temperatures (°F)	61	62	69	68	70	67	72	69

Entering Air Temperature: ESP-=0.3 in wg @ 55°F – Data Center Room												
Rack Type	5.5KW		5.5KW		5.5KW		5.5KW		5.5KW		5.5KW	
Entering points	Q	S	U	W	Y	AA	EE	CC	II	GG	MM	KK
EAT Display temperatures (°F)	76	69	70	69	78	68	69	74	69	74	66	72

Leaving Air Temperature Analysis: ESP-=0.3 in wg @ 55°F										
Room	Scada				Data Center					
Tagged Point	1--4	5--8	9--12	13--16	17--20	21--24	25--28	29--32	33-36	37--40
Leaving Air Temperature behind the Rack (°F)	72.17	87.62	96.31	90.33	88.63	87.87	91.06	87.55	92.82	92.31
	69.37	99.83	94.74	95.28	102.20	93.29	96.41	97.17	95.42	87.43
	61.43	95.78	88.15	95.64	93.30	82.45	85.14	81.85	80.69	73.65
	64.36	104.32	92.13	96.59	87.06	90.55	86.15	86.40	88.15	68.55
	69.60	105.70	100.88	92.09	86.52	93.19	94.33	93.44	92.18	81.18
	64.47	81.31	78.02	76.67	82.99	78.22	79.79	79.44	78.96	77.22
	65.66	80.25	83.13	78.09	80.55	82.01	78.66	80.75	83.96	79.31
	73.35	111.14	113.68	99.78	108.31	109.37	104.98	114.02	115.17	82.20
	65.66	104.09	95.31	91.76	91.19	89.83	93.10	94.98	93.22	77.30
	62.98	98.19	92.70	92.54	84.41	86.37	87.60	88.48	88.51	73.00
	68.62	105.33	97.43	100.86	97.50	98.65	97.87	97.71	99.36	75.33
	64.82	81.19	79.30	77.72	75.81	76.56	82.69	79.05	77.92	75.26
	62.76	73.10	73.46	71.28	72.69	73.91	72.16	73.06	74.88	72.38
	70.86	96.78	102.38	88.43	95.93	100.01	92.06	95.58	97.45	88.03
	69.00	91.72	87.09	89.31	88.49	87.15	91.70	90.39	88.78	84.18
	60.58	69.80	70.53	68.45	69.46	69.34	72.11	70.78	70.66	70.23
	62.03	72.52	75.08	68.00	74.84	77.30	69.02	72.82	76.73	70.12
	78.98	108.43	117.12	108.93	113.67	119.11	121.10	118.54	118.69	101.41
	76.79	110.32	105.82	106.79	108.08	109.99	111.26	109.96	109.39	100.66
	72.26	102.54	106.76	106.30	110.95	110.78	110.00	110.05	111.01	92.18
	71.52	96.86	95.75	97.54	98.66	95.22	103.08	96.92	96.48	86.89

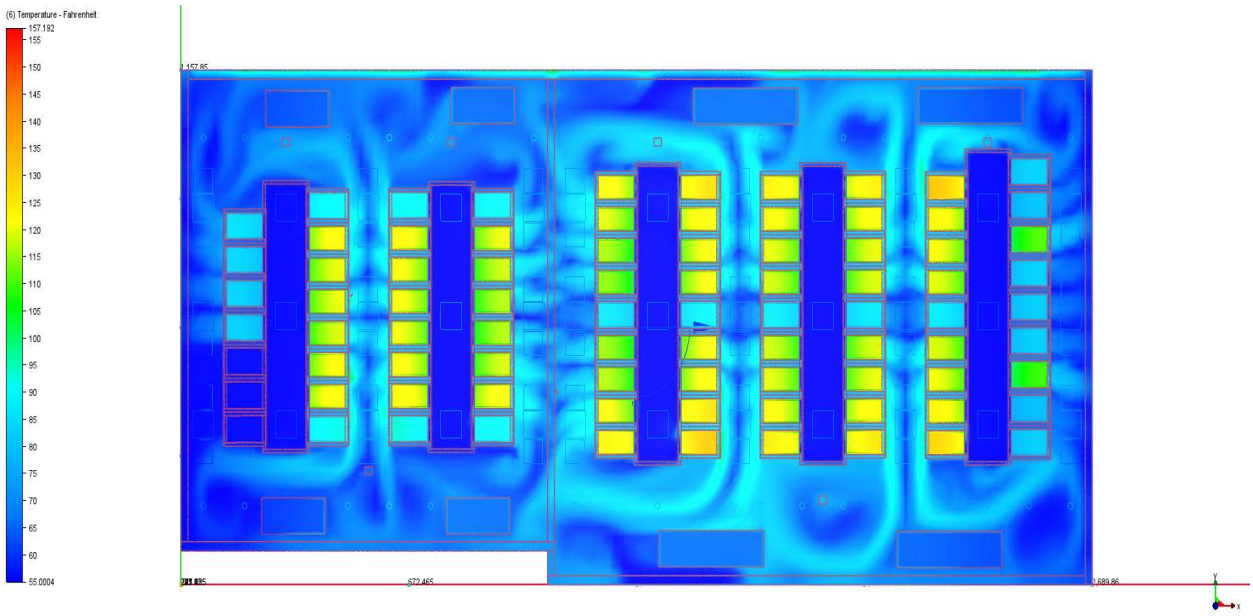

Figure 4.2 The temperature distribution at 5 foot above ground level (ESP=0.4 IN WG, LAT=55°F)

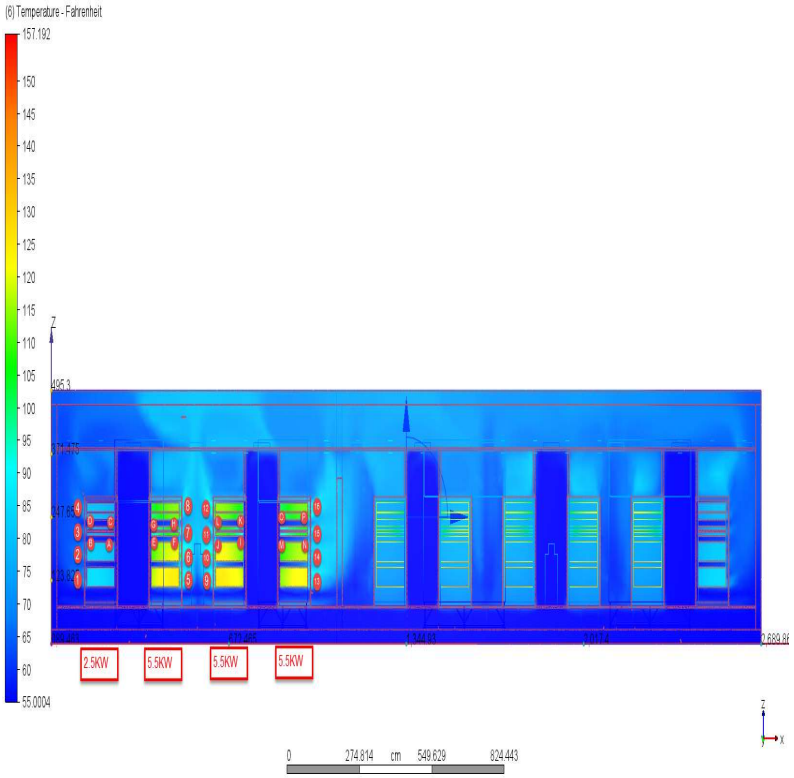

Figure 4.2a
Section View in Scada Room (ESP=0.4 IN WG, LAT=55°F)

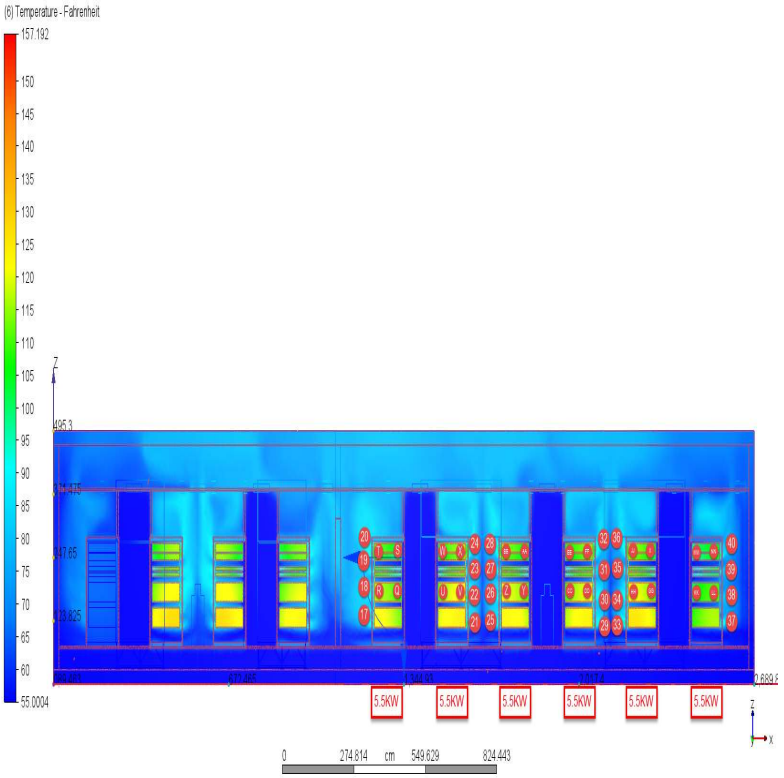

Figure 4.2b
Section View in Data Center Room (ESP=0.4 IN WG, LAT=55°F)

Entering Air Temperature: ESP-=0.4 in wg @ 55°F - Scada Room								
Rack Type	2.5kw		5.5KW		5.5KW		5.5KW	
Entering points	A	C	E	G	M	O	I	K
EAT Display temperatures (°F)	62	62	68	69	61	67	63	65

Entering Air Temperature: ESP-=0.4 in wg @ 55°F – Data Center Room												
Rack Type	5.5KW		5.5KW		5.5KW		5.5KW		5.5KW		5.5KW	
Entering points	Q	S	U	W	Y	AA	EE	CC	II	GG	MM	KK
EAT Display temperatures (°F)	68	67	68	66	78	68	68	72	68	69	63	68

Leaving Air Temperature Analysis: ESP-=0.4 in wg @ 55°F										
Room	Scada				Data Center					
Tagged Point	1--4	4--8	9--12	13--16	17--20	21--24	25--28	29--32	33--36	37--40
Leaving Air Temperature behind the Rack (°F)	73.33	90.89	89.16	90.58	83.26	89.45	82.47	89.81	82.06	83.77
	77.99	95.47	89.63	94.79	94.61	99.13	92.92	94.33	96.76	91.73
	66.98	95.61	85.65	95.32	91.58	91.79	82.09	83.77	85.92	87.18
	68.66	101.80	90.15	86.05	92.91	86.80	87.24	84.31	88.83	69.22
	71.57	91.93	99.54	90.21	88.07	88.02	91.89	90.47	97.72	84.02
	63.09	79.55	77.13	77.34	76.24	80.79	78.27	78.78	80.35	75.40
	65.17	82.23	82.52	83.64	77.75	79.50	78.92	79.52	77.09	80.16
	76.45	107.42	109.53	89.52	96.40	107.76	104.85	103.57	107.12	79.76
	69.53	97.93	92.05	87.39	88.34	87.89	88.12	87.10	91.73	76.38
	67.02	92.46	90.57	87.79	88.40	83.38	82.12	84.14	89.42	72.19
	71.39	100.17	91.89	88.18	96.90	95.10	94.52	96.36	103.82	76.68
	62.87	73.90	79.44	79.26	73.84	75.08	76.36	76.75	78.97	75.14
	61.86	75.94	71.77	69.78	72.69	72.50	71.97	71.65	72.04	72.11
	71.33	94.64	94.83	89.73	90.02	92.58	95.18	91.07	91.17	87.14
	68.33	83.93	86.75	86.31	78.58	83.64	82.56	85.45	85.91	78.39
	60.17	68.54	68.21	67.52	67.19	69.30	68.90	70.15	69.87	67.54
	62.40	81.60	71.05	72.55	82.33	77.95	78.45	74.42	72.50	77.77
	81.16	105.00	112.17	106.56	108.15	112.96	104.23	110.88	107.64	103.66
	76.17	104.63	106.36	102.29	101.59	106.08	107.24	106.58	106.44	97.62
	75.76	95.60	104.17	98.67	99.86	109.55	107.20	107.26	105.55	91.36
	70.30	88.75	93.34	92.90	85.17	92.93	89.85	92.96	90.17	83.32

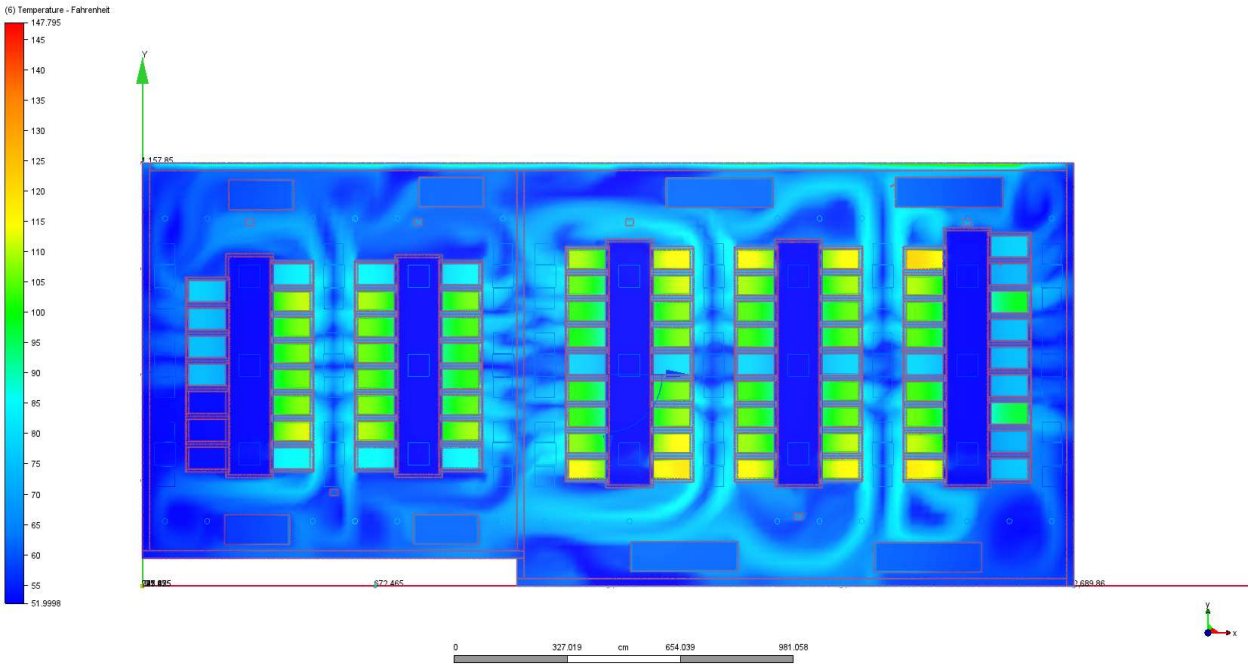

Figure 4.3 The temperature distribution at 5 foot above ground level (ESP=0.5 IN WG, LAT=55°F)

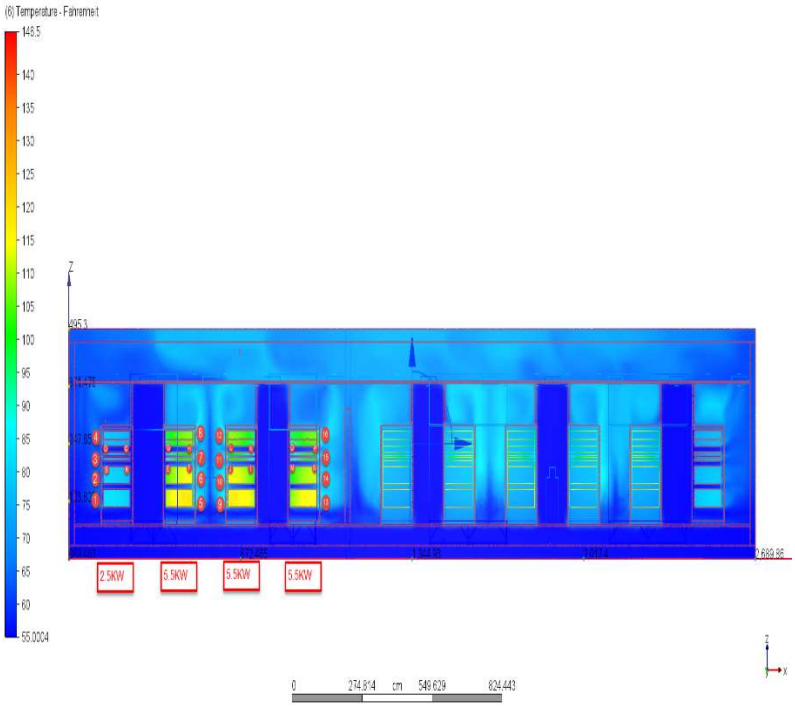

Figure 4.3a
Section View in Scada Room (ESP=0.5 IN WG, LAT=55°F)

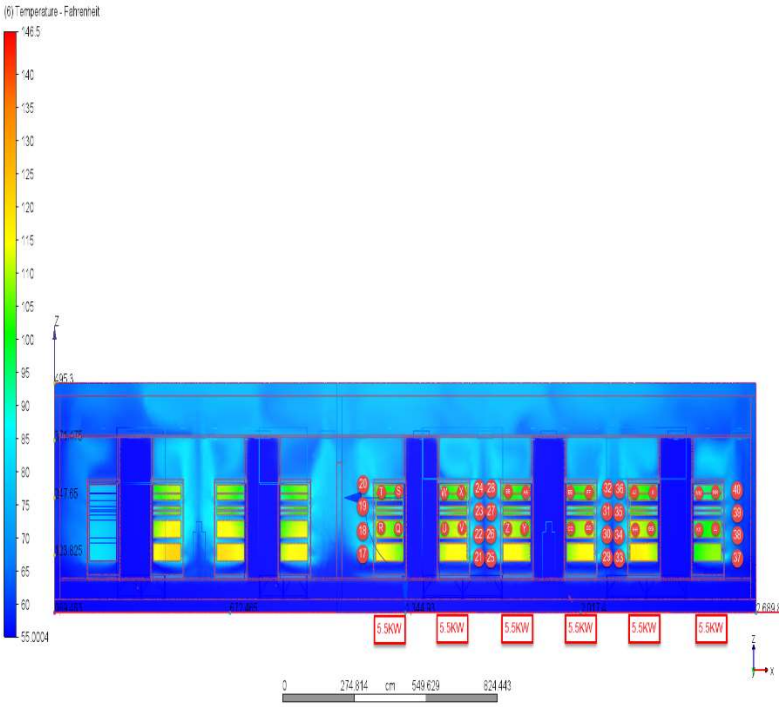

Figure 4.3b
Section View in Data Center Room (ESP=0.5 IN WG, LAT=55°F)

Entering Air Temperature: ESP-=0.5 in wg @ 55°F - Scada Room								
Rack Type	2.5kw Rack		5.5kw Rack		5.5kw Rack		5.5kw Rack	
Entering points	A	C	E	G	M	O	I	K
EAT Display temperatures (°F)	62	61	66	65	72	68	75	74

Entering Air Temperature: ESP-=0.5 in wg @ 55°F – Data Center Room												
Rack Type	5.5KW		5.5KW		5.5KW		5.5KW		5.5KW		5.5KW	
Entering points	Q	S	U	W	Y	AA	EE	CC	II	GG	MM	KK
EAT Display temperatures (°F)	69	60	64	60	72	66	60	71	60	68	60	64

Leaving Air Temperature Analysis: ESP-=0.5 in wg @ 55°F										
Room	Scada				Data Center					
Tagged Point	1--4	5--8	9--12	13--16	17--20	21--24	25--28	29--32	33--36	37--40
Leaving Air Temperature behind the Rack (°F)	69.73	86.43	82.50	84.98	90.53	94.79	94.78	96.14	87.91	91.87
	64.69	90.55	89.16	87.74	86.75	89.31	83.58	80.18	101.76	93.52
	62.01	83.95	82.67	86.39	86.68	84.19	76.52	74.19	89.40	79.21
	60.87	89.83	84.47	88.00	90.67	78.52	84.72	81.58	93.39	62.84
	65.13	92.27	84.91	87.24	87.21	80.13	82.75	79.80	93.99	75.27
	62.70	74.89	75.09	73.69	71.45	75.07	72.88	73.18	73.33	72.56
	64.28	80.30	74.88	78.78	74.29	78.85	76.43	79.86	74.16	79.45
	70.44	95.31	89.65	84.59	97.77	97.92	97.14	94.67	103.28	80.75
	67.50	91.37	89.64	81.91	92.71	82.23	82.79	81.82	92.44	83.68
	63.22	86.25	83.37	86.27	90.51	80.36	80.68	82.88	87.36	72.74
	68.14	92.00	86.48	84.93	93.91	89.26	87.22	90.85	92.32	74.66
	67.30	81.40	77.28	73.16	73.20	69.97	73.77	71.47	77.03	68.71
	60.99	69.41	68.73	69.52	66.95	69.59	67.20	70.48	67.91	71.96
	67.26	87.36	88.40	86.59	82.05	89.21	85.85	87.29	85.57	81.48
	67.95	85.19	83.93	79.34	82.63	80.50	84.24	79.02	85.52	75.13
	61.88	66.97	66.40	65.78	64.50	66.18	67.22	66.45	67.32	66.37
	59.41	69.67	66.41	74.54	64.39	70.60	64.26	71.86	64.09	73.86
	75.12	104.60	100.64	101.04	100.96	98.30	96.65	99.31	94.64	94.86
	74.95	100.79	101.04	100.23	97.25	97.54	99.05	97.43	98.71	87.56
	72.69	99.23	100.48	95.93	99.00	97.02	98.43	95.94	101.29	82.82
	71.16	97.64	91.29	87.88	92.59	89.51	93.91	87.93	93.98	83.37

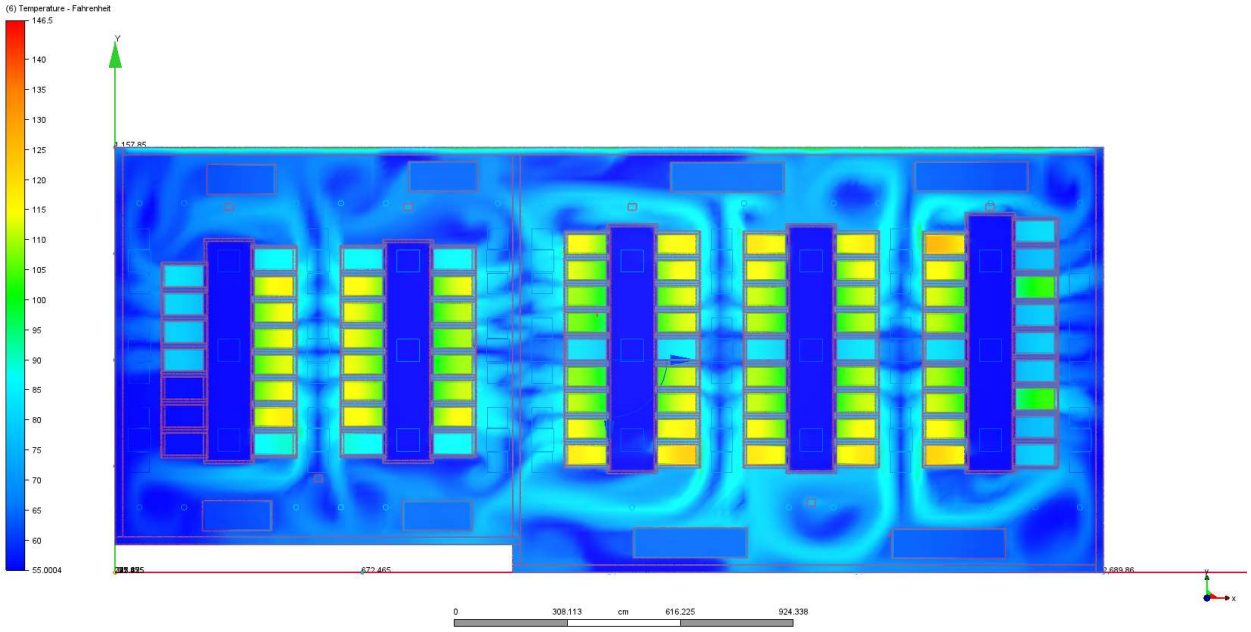

Figure 4.4 The temperature distribution at 5 foot above ground level (ESP=0.5 IN WG, LAT=52°F)

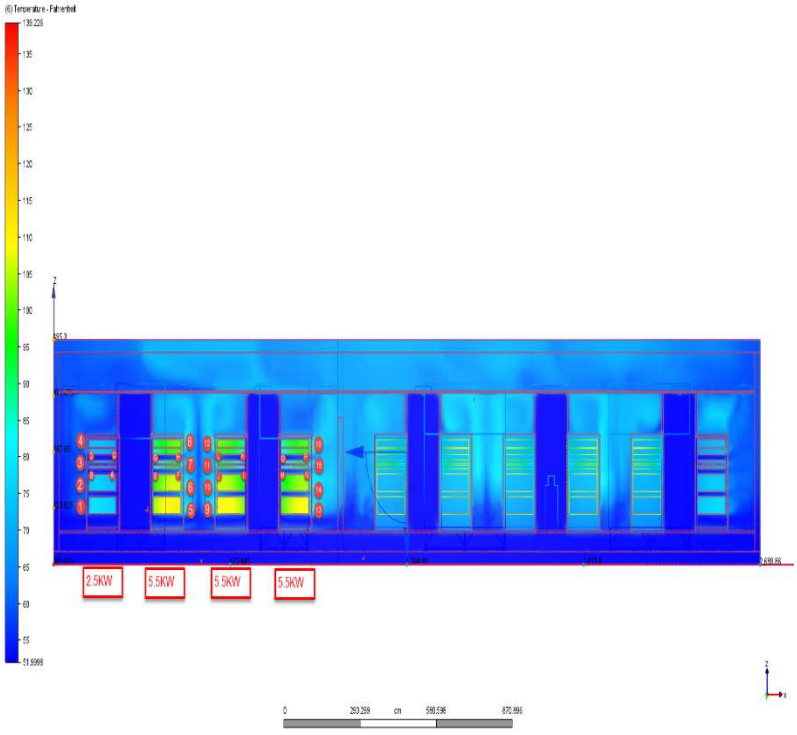

Figure 4.4a
Section View in Scada Room (ESP=0.5 IN WG, LAT=52°F)

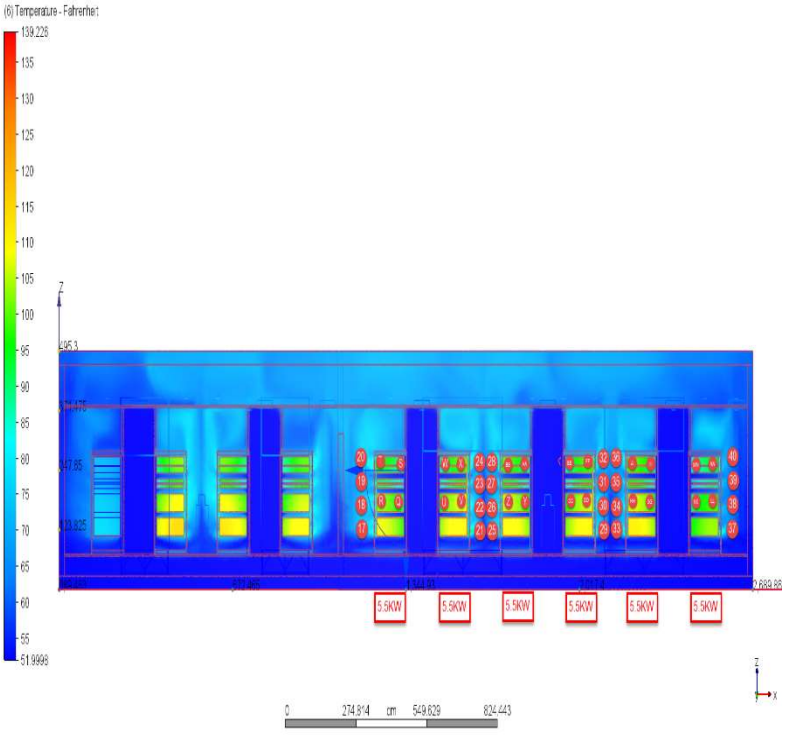

Figure 4.4b
Section View in Data Center Room (ESP=0.5 IN WG, LAT=52°F)

Entering Air Temperature: ESP-=0.5 in wg @ 52°F - Scada Room								
Rack Type	2.5kw		5.5kw		5.5kw		5.5kw	
Entering points	A	C	E	G	M	O	I	K
EAT Display temperatures (°F)	60	60	65	63	70	60	72	64

Entering Air Temperature: ESP-=0.5 in wg @ 52°F – Data Center Room												
Rack Type	5.5KW		5.5KW		5.5KW		5.5KW		5.5KW		5.5KW	
Entering points	Q	S	U	W	Y	AA	EE	CC	II	GG	MM	KK
EAT Display temperatures (°F)	68	62	68	60	68	62	60	68	60	68	59	64

Leaving Air Temperature Analysis: ESP-=0.5 in wg @ 52°F										
Room	Scada				Data Center					
Tagged Point	1--4	5--8	9--12	13--16	17--20	21-24	25--28	29--32	32--36	37--40
Leaving Air Temperature behind the Rack (°F)	65.22	89.23	89.88	95.92	90.37	75.34	96.97	87.78	86.74	94.68
	65.25	87.55	87.61	91.08	87.99	69.20	98.69	99.25	92.80	97.64
	65.15	85.54	83.09	81.69	84.16	64.65	88.87	92.15	88.83	93.60
	63.52	82.99	80.53	81.11	82.69	32.00	88.91	86.86	85.65	96.58
	61.67	80.84	79.27	82.32	84.76	62.57	97.87	86.39	81.44	96.76
	60.69	79.01	77.74	83.91	86.81	62.65	96.69	85.72	77.14	96.98
	59.99	78.52	77.14	87.34	87.37	63.12	97.60	85.20	73.07	97.21
	59.29	78.77	79.34	90.72	86.65	63.68	99.94	84.98	73.90	97.47
	59.06	79.06	81.54	90.29	85.92	64.17	85.29	83.34	77.82	97.74
	59.91	81.15	84.78	89.04	85.14	64.63	73.24	82.23	82.28	98.04
	60.02	84.56	82.76	87.62	80.63	64.95	79.21	81.43	86.06	98.35
	59.83	88.33	80.01	86.33	75.30	65.24	85.11	81.25	83.74	98.69
	59.39	83.23	76.93	84.48	69.96	65.42	90.93	80.58	78.81	99.04
	58.93	77.53	70.31	83.76	67.27	65.58	94.70	79.82	73.88	99.30
	58.99	71.83	69.60	68.00	66.34	65.60	70.91	69.81	69.61	99.41
	59.25	69.70	68.83	67.11	66.67	65.63	68.73	68.96	68.35	99.51
	59.83	68.66	71.94	67.15	73.16	65.85	67.73	68.06	67.44	99.58
	60.41	69.38	77.17	81.66	79.49	66.06	87.04	76.17	69.94	99.63
	61.26	78.93	82.48	87.53	85.38	65.93	92.49	82.87	78.16	99.18
	61.86	88.45	87.26	93.22	83.48	66.80	97.97	89.79	87.26	98.65
	62.84	94.84	91.19	94.33	80.90	67.53	99.15	95.77	95.21	97.86

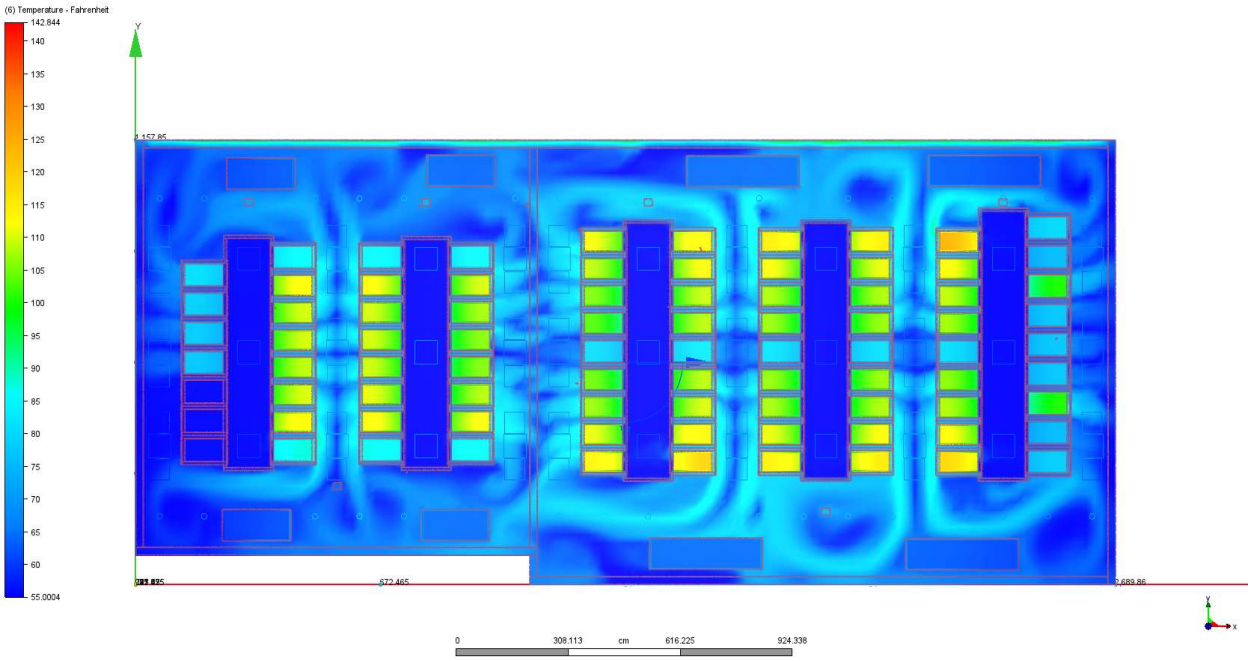

Figure 4.5 The temperature distribution at 5 foot above ground level (ESP=0.6 IN WG, LAT=55°F)

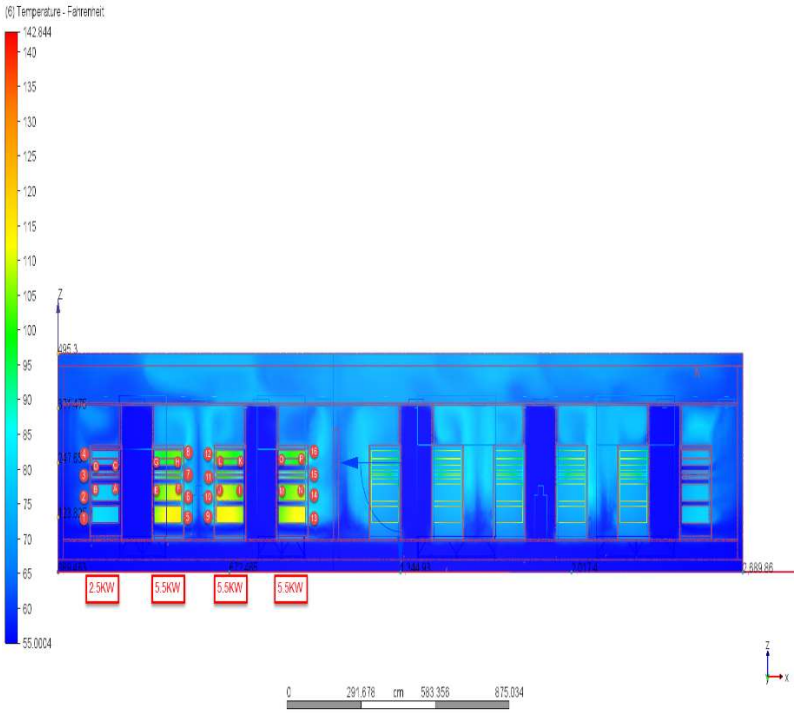

Figure 4.5a
Section View in Scada Room (ESP=0.6 IN WG, LAT=55°F)

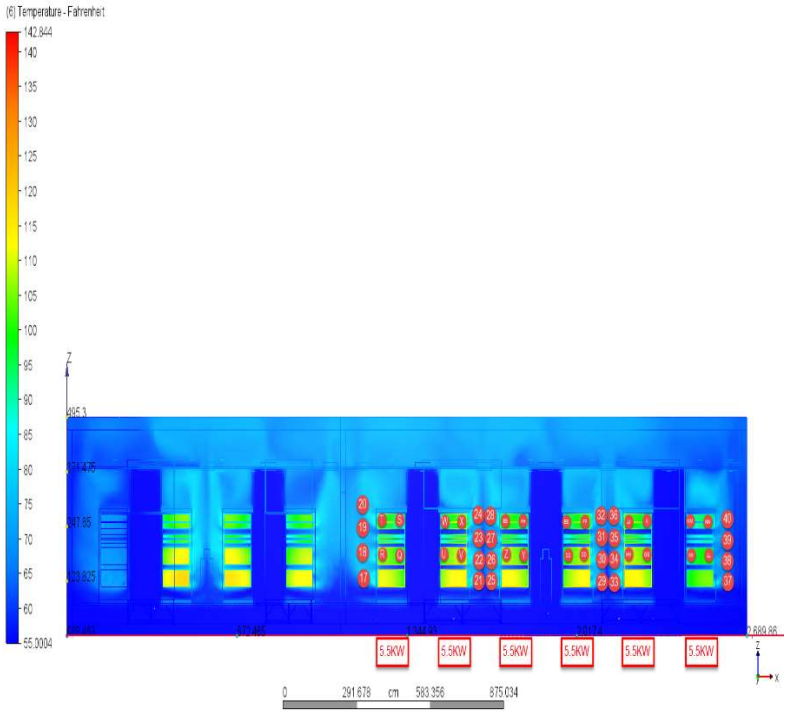

Figure 4.5b
Section View in Data Center Room (ESP=0.6 IN WG, LAT=55°F)

Entering Air Temperature: ESP-=0.6 in wg @ 55°F - Scada Room								
Rack Type	2.5kw		5.5kw		5.5kw		5.5kw	
Entering points	A	C	E	G	M	O	I	K
EAT Display temperatures (°F)	60	59	61	60	64	60	68	62

Entering Air Temperature: ESP-=0.6 in wg @ 55°F – Data Center Room												
Rack Type	5.5KW		5.5KW		5.5KW		5.5KW		5.5KW		5.5KW	
Entering points	Q	S	U	W	Y	AA	EE	CC	II	GG	MM	KK
EAT Display temperatures (°F)	64	60	68	62	64	62	63	68	60	69	60	68

Leaving Air Temperature Analysis: ESP-=0.6 in wg @ 55°F										
Room	Scada				Data Center					
Tagged Point	1--4	5--7	9--12	13--16	17--20	21--24	25--28	29--32	33-36	37--40
Leaving Air Temperature behind the Rack (°F)	68.86	86.62	85.32	90.24	84.16	94.39	89.24	90.64	92.35	94.39
	66.29	92.97	92.40	95.21	90.71	93.36	83.35	79.79	94.05	95.07
	65.46	88.84	93.95	86.19	94.49	94.44	82.25	73.53	86.33	81.64
	65.48	84.90	91.61	80.59	93.75	81.78	86.86	78.69	94.07	66.29
	65.47	82.63	89.63	84.15	91.02	85.32	85.58	82.97	89.13	81.93
	64.46	81.38	87.63	87.48	88.28	75.00	71.36	72.38	71.45	70.41
	62.55	80.88	85.57	90.50	85.55	81.65	77.35	73.34	76.79	82.20
	60.94	80.99	84.99	93.13	83.74	94.14	94.22	93.28	94.95	79.65
	61.28	81.62	84.46	91.62	83.08	94.98	92.61	85.29	90.88	81.15
	62.36	85.36	83.92	91.46	82.46	86.31	80.35	81.13	83.98	67.91
	62.87	90.09	83.39	92.35	81.84	91.59	89.77	89.65	95.29	76.20
	63.29	91.19	82.63	92.56	81.22	82.61	76.57	76.63	72.98	68.50
	63.30	84.98	81.84	90.10	80.57	66.34	66.11	66.88	67.56	70.63
	62.63	78.57	81.14	87.25	79.92	81.70	80.85	79.93	82.59	80.38
	61.72	74.93	82.12	71.96	79.44	83.85	81.65	81.11	79.43	77.50
	62.19	72.92	83.09	70.45	80.94	74.09	70.40	66.81	65.86	64.29
	64.54	71.97	84.07	70.43	82.45	64.66	62.13	64.20	64.29	67.51
	66.89	79.45	84.81	85.21	83.96	94.89	94.99	94.05	94.16	95.62
	69.63	86.92	86.45	89.44	85.47	94.13	94.93	94.77	94.98	90.87
	68.38	91.35	88.09	93.55	87.09	94.46	94.45	94.21	94.81	88.82
	66.15	90.04	89.74	95.54	88.79	93.89	94.18	94.80	92.64	83.34

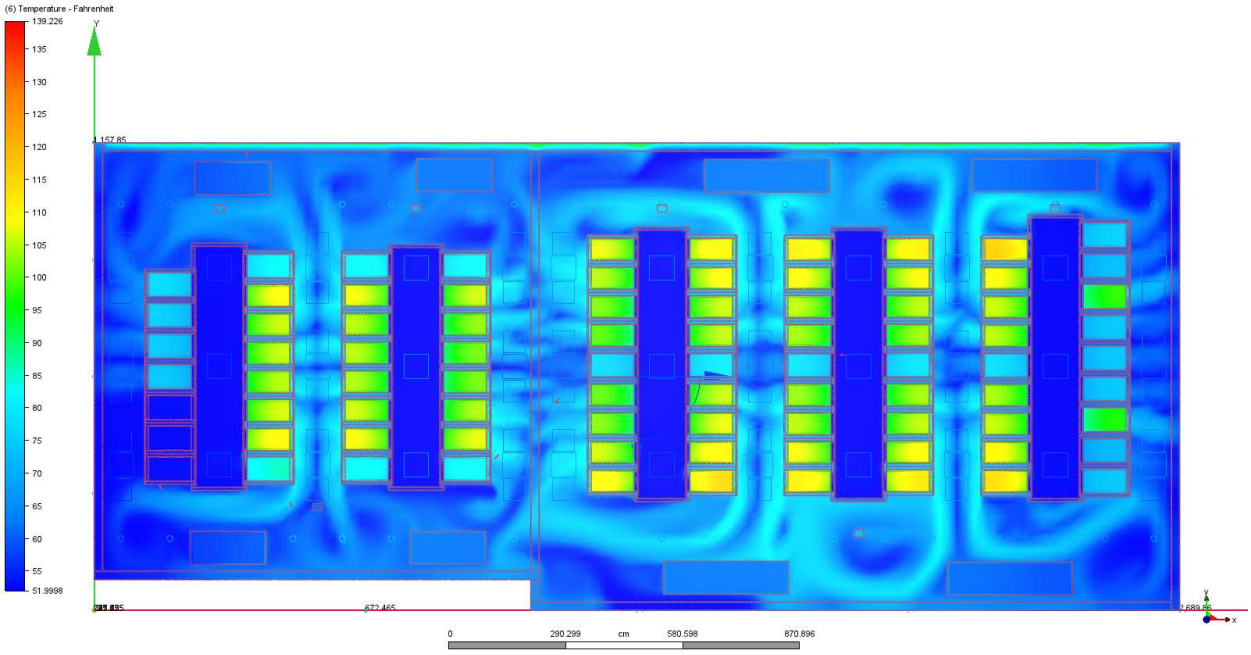

Figure 4.6 The temperature distribution at 5 foot above ground level (ESP=0.6 IN WG, LAT=52°F)

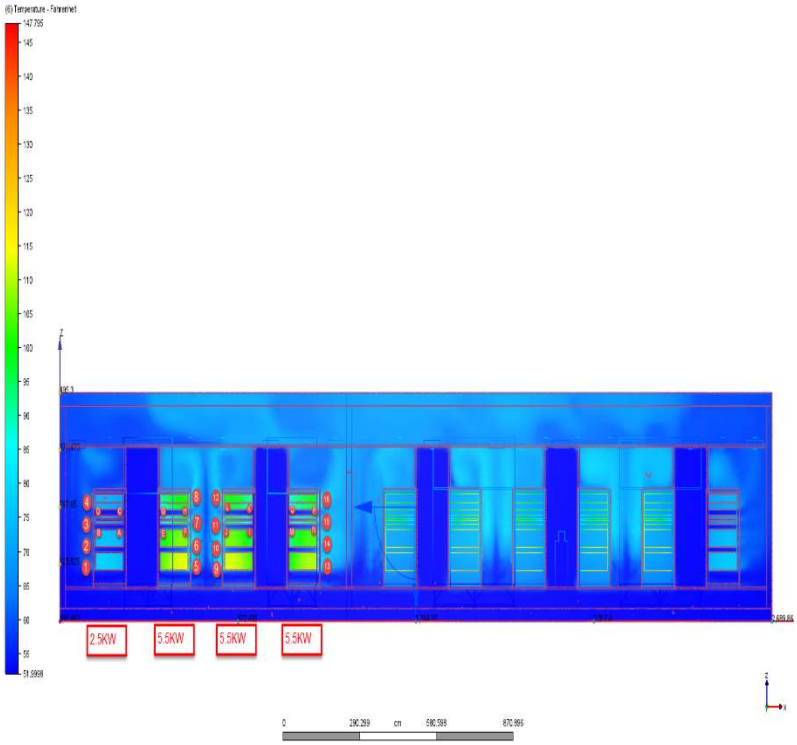

Figure 4.6a
Section View in Scada Room (ESP=0.6 IN WG, LAT=52°F)

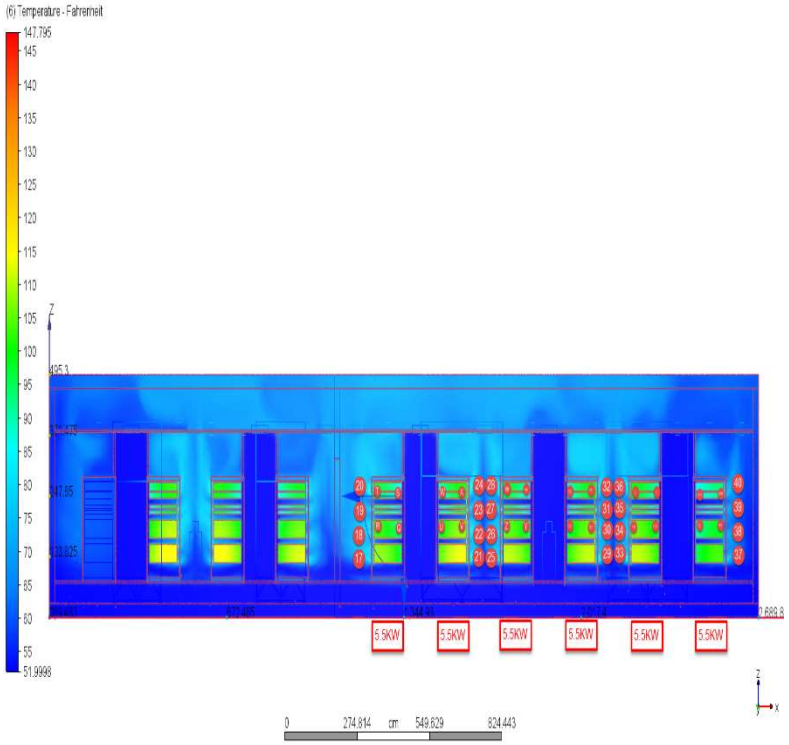

Figure 4.6b
Section View in Data Center Room (ESP=0.6 IN WG, LAT=52°F)

Entering Air Temperature: ESP-=0.6 in wg @ 52°F - Scada Room								
Rack Type	2.5KW		5.5KW		5.5KW		5.5KW	
Entering points	A	C	E	G	M	O	I	K
EAT Display temperatures (°F)	59	59	60	60	63	62	67	60

Entering Air Temperature: ESP-=0.6 in wg @ 52°F – Data Center Room												
Rack Type	5.5KW		5.5KW		5.5KW		5.5KW		5.5KW		5.5KW	
Entering points	Q	S	U	W	Y	AA	EE	CC	II	GG	MM	KK
EAT Display temperatures (°F)	62	60	64	60	63	60	62	66	60	66	60	65

Leaving Air Temperature Analysis: ESP-=0.6 in wg @ 52°F										
Room	Scada				Data Center					
Tagged Point	61.51	69.79	66.89	68.52	74.89	73.84	73.18	60.83	74.57	68.35
Leaving Air Temperature behind the Rack (°F)	64.68	87.12	81.69	77.76	78.18	87.60	81.65	79.58	85.14	78.52
	60.79	79.33	81.04	75.30	75.77	80.70	75.41	84.66	79.21	72.10
	58.66	75.30	78.09	75.10	77.22	72.58	73.69	75.27	73.89	64.74
	59.76	73.40	75.67	74.27	75.24	74.34	72.58	73.42	73.17	69.45
	59.35	70.91	71.08	70.32	69.34	70.46	71.04	72.22	71.81	67.91
	60.77	76.36	72.10	71.97	72.84	75.83	72.83	71.57	73.81	70.05
	61.61	80.22	77.38	76.91	78.09	81.25	78.84	75.93	79.40	72.18
	60.36	78.26	78.59	74.13	76.35	80.87	75.61	80.12	77.34	67.12
	59.39	74.97	75.15	75.02	76.81	76.74	73.62	76.18	74.72	62.09
	60.07	70.51	72.97	71.97	74.67	75.10	73.38	73.58	74.23	66.47
	58.43	68.85	67.54	68.31	67.04	66.83	69.03	72.51	69.67	65.66
	60.39	71.78	70.61	69.76	71.16	69.89	67.25	66.32	69.41	69.47
	62.26	73.86	72.58	73.94	74.78	77.63	76.59	71.64	73.35	72.18
	58.20	63.70	69.49	66.57	65.28	69.65	70.64	73.20	72.96	64.57
	57.18	68.90	65.21	65.33	63.78	63.38	62.67	67.74	64.58	62.23
	61.74	75.27	68.99	76.29	76.10	72.71	66.88	64.28	66.19	75.02
	64.86	81.28	76.89	81.48	83.47	84.46	79.62	73.80	75.22	78.24
	63.87	81.81	81.32	80.35	81.46	86.93	81.78	80.66	79.32	75.16
	62.78	75.46	80.10	75.92	76.56	83.83	82.29	83.10	80.73	72.57
	60.26	73.52	73.73	66.49	69.90	73.30	74.59	80.46	75.64	66.09
	57.18	63.70	65.21	65.33	63.78	63.38	62.67	60.83	64.58	62.09

Table 1 provides a presentation of outcomes for multiple scenarios, corresponding to the thermal map as shown in **Figure 4**. These scenarios include a range of Leaving Air Temperatures (LAT) from 52 to 55 °F and External Static Pressures (ESP) spanning 0.2 to 0.6 (in.wg) for Day Two situations. Upon analyzing the summarized data in **Table 1**, it appears that compliance with the design requirements for equipment environment specifications within the data center, particularly for server racks, is achieved only when specifying a CRAC unit configuration with an ESP of 0.6 and a LAT of 52 °F. It is worth noting that with the revised CRAC unit configuration (ESP of 0.6 and LAT of 52 °F), the output result of thermal distribution for Day One operation (approximately 61.4% operational load) also complies with the permissible temperature specified for server racks.

Entering Air Temperature (EAT) Analysis Summary Table for IT Racks							
Scenarios	ESP=0.2@55F	ESP=0.3@55F	ESP=0.4@55F	ESP=0.5@55F	ESP=0.5@52F	ESP=0.6@55F	ESP=0.6@52F
Minimum (°F)	61	61	61	60	59	59	59
Average (°F)	70	70	67	66	64	63	62
Maximum (°F)	77	78	78	75	72	69	67

Leaving Air Temperature (LAT) Analysis Summary Table for IT Racks										
Room	Scada				Data Center					
Rack Type	2.5kW	5.5kW	5.5kW	5.5kW	5.5kW	5.5kW	5.5kW	5.5kW	5.5kW	5.5kW
TAGED POINT	1--4	5--8	9--12	13--16	17--20	21--24	25--28	29--32	33--36	37--40
ESP=0.2@55°F	81.08	123.88	122.44	119.64	122.72	126.19	130.71	122.91	132.64	110.94
ESP=0.3@55°F	78.98	111.14	117.12	108.93	113.67	119.11	121.10	118.54	118.69	101.41
ESP=0.4@55°F	81.16	107.42	112.17	106.56	108.15	112.96	107.24	110.88	107.64	103.66
ESP=0.5@55°F	75.12	104.60	101.04	101.04	100.96	98.30	99.05	99.31	103.28	94.86
ESP=0.5@52°F	65.25	94.84	91.19	95.92	90.37	75.34	99.94	99.25	95.21	99.63
ESP=0.6@55°F	69.63	92.97	93.95	95.54	94.49	94.98	94.99	94.80	95.29	95.62
ESP=0.6@52°F	64.86	87.12	81.69	81.48	83.47	87.60	82.29	84.66	85.14	78.52

Table 1: Temperature Analysis Summary Table for IT Racks							
Scenarios	ESP=0.2@55F	ESP=0.3@55F	ESP=0.4@55F	ESP=0.5@55F	ESP=0.5@52F	ESP=0.6@55F	ESP=0.6@52F
EAT (°F)	61	61	61	60	59	59	59
LAT (°F)	132.64	121.10	112.96	104.60	99.94	95.62	87.60
ASHRAE Temperature Allowable 59 °F- 89.6°F	Fail	Fail	Fail	Fail	Fail	Fail	Pass

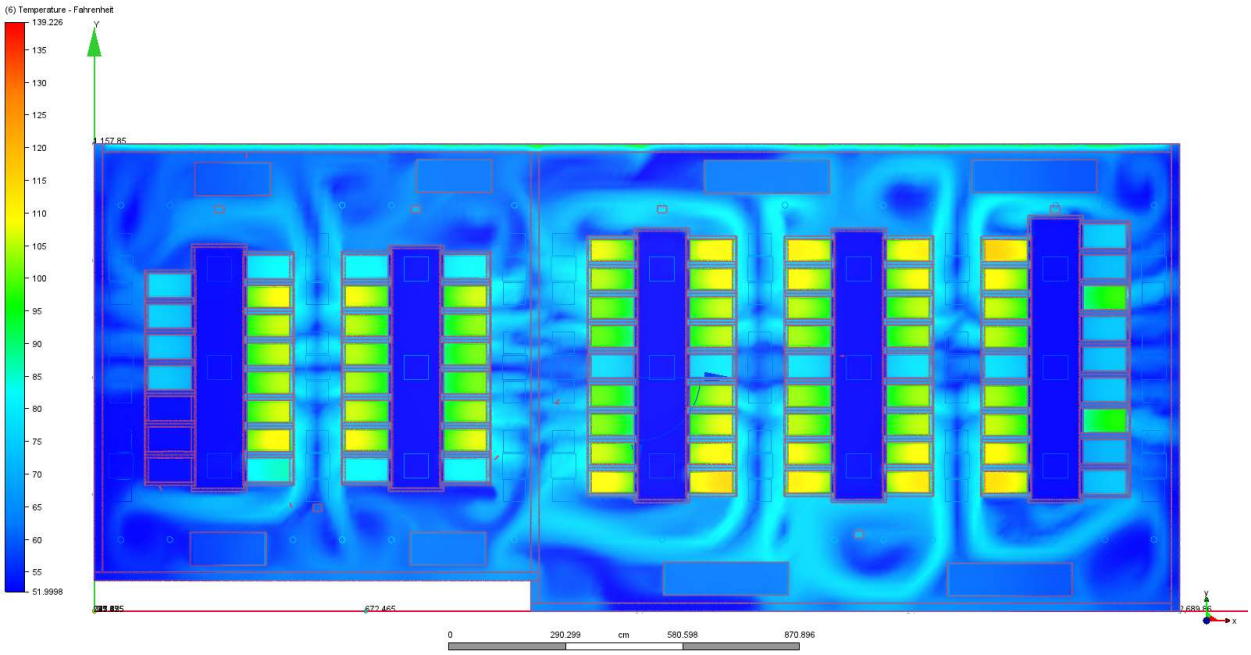

Figure 5.1 The temperature distribution at 5 feet above ground level (ESP=0.6 IN WG, LAT=52°F)

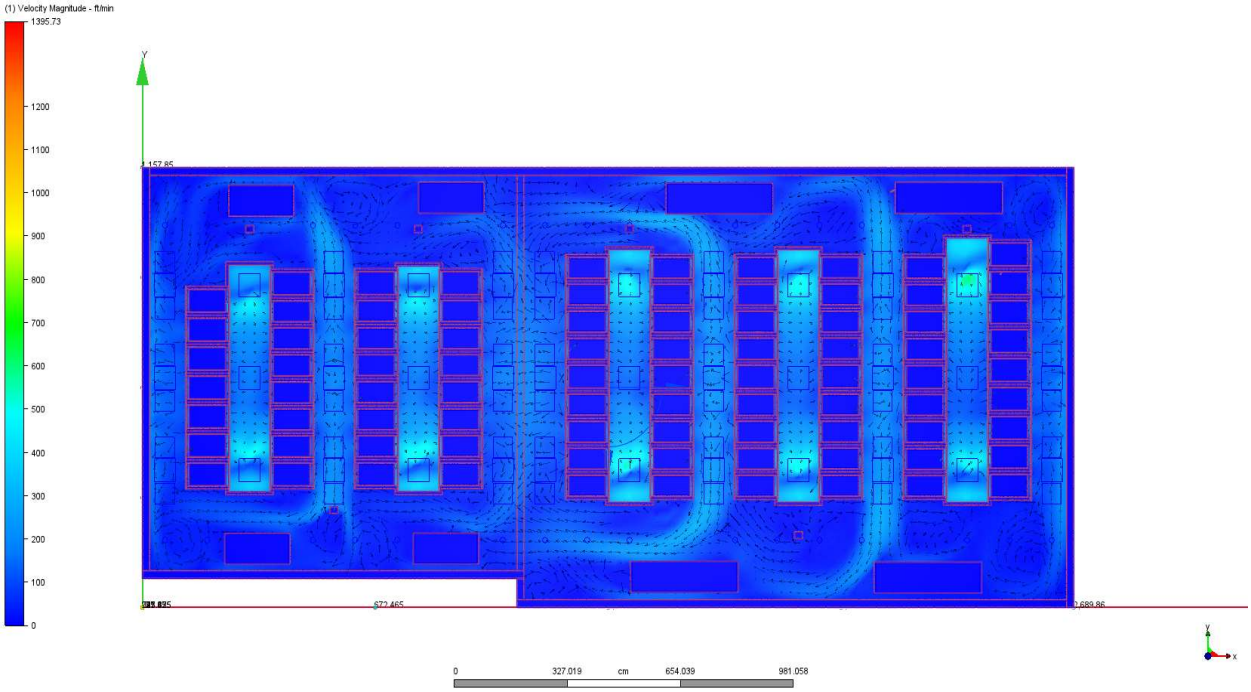

Figure 5.2 The velocity distribution at 5 feet above ground level (ESP=0.6 IN WG, LAT=52°F)

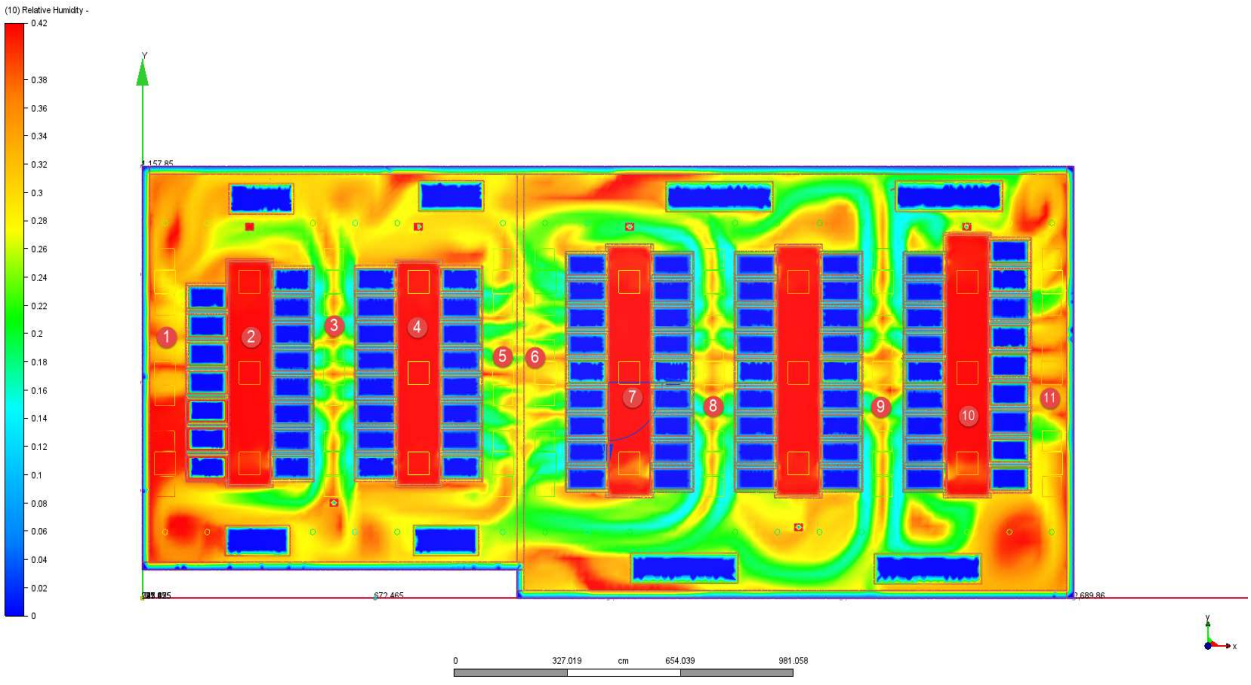

Figure 5.3 The relative humidity distribution at 5 feet above ground level (ESP=0.6 IN WG, LAT=52°F)

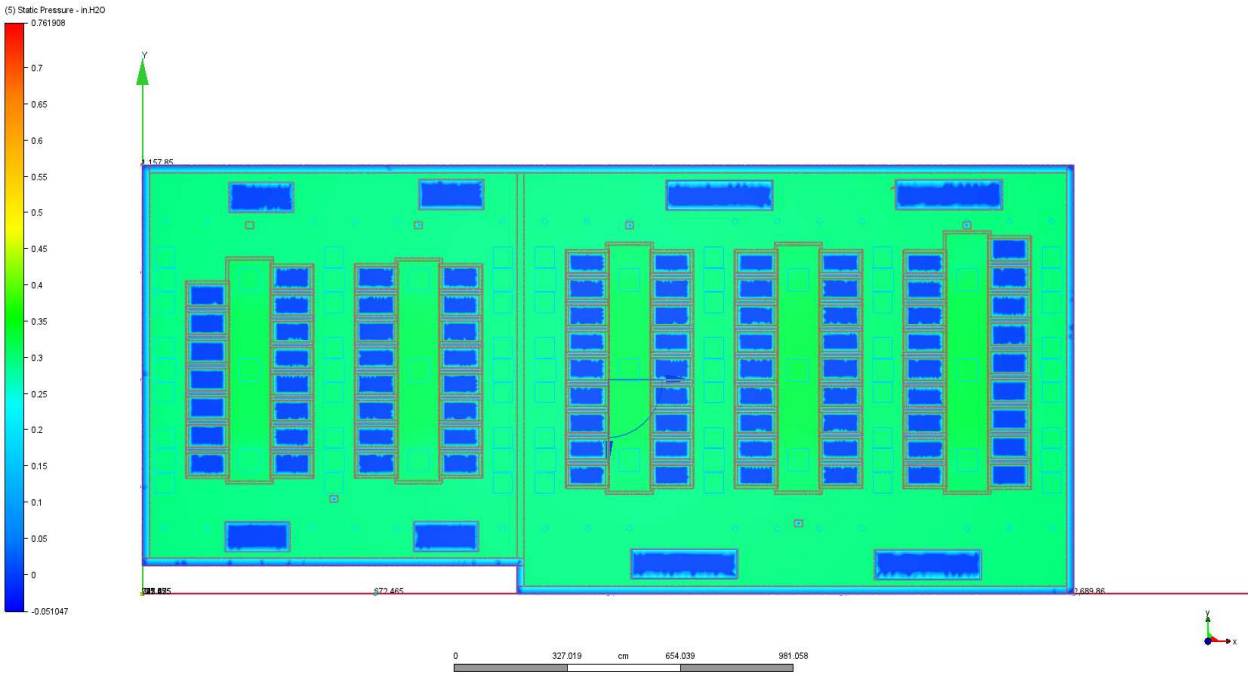

Figure 5.4 The static pressure distribution at 5 feet above ground level (ESP=0.6 IN WG, LAT=52°F)

As shown in **Figure 5** above**,** the data center, equipped with CRAC units specified with an ESP of 0.6 and a LAT of 52 °F, demonstrates compliance to the acceptable temperature limits for server racks. Also, the humidity and static pressure/velocity distributions align with the specified design criteria. The humidity ranges from 34% to 42% relative humidity (RH), satisfying the design criteria below 60% RH. The average static pressure is 0.375 in wg, and the velocity ranges from 200 to 300 fpm, both of which are within acceptable parameters.

Case Study 2

Validating Ventilation Systems in Hospital Operating Rooms (OR)

Clarksville, Texas

Hospital operating rooms introduce a distinctive array of complexities when it comes to the design and validation of ventilation systems. The impacts of system failure in these critical settings can be life-saving or life-threatening, emphasizing the criticality of adherence to stringent design criteria and health care standards. These criteria include the precise control of temperature and humidity, precise management of airborne contaminants, and the establishment of correct airflow patterns that not only meet strict sterility requirements but also ensure a comfortable environment for surgical teams. The design and validation of such ventilation systems heavily relied on health care codes and standards, engineering guidelines, and experiential knowledge. However, the limitations of the design methods, particularly in delivering the required precision and assurance demanded by contemporary healthcare facilities, have underscored the need for more advanced solutions. This is precisely where Computational Fluid Dynamics (CFD) analysis appears as a powerful tool in the validation of hospital operating room ventilation systems.

In this case study, we develop CFD analysis to examine the OR ventilation system of a newly constructed 32,920 square foot, 23-bed hospital in Clarksville, Texas, as shown in **Figure 1**. The OR in this study has an operating table, a patient, two surgeons, two nurses, an anesthesiologist, surgical lights, can lights, square lights, computers, monitors, anesthesia machines. The sensible heat load for occupants is calculated to be 1,500 Btu/h. The sensible heat load for all lights is assumed to be 1,940 Btu/h. The sensible heat load for computers, monitors, and other equipment is assumed to be 2,903 Btu/h. The exterior wall and roof &ceiling sensible heat loads are assumed to be 815 Btu/h and 2,986 Btu/h, respectively. The total sensible heat load within the OR is assumed to be 10,144 Btu/h.

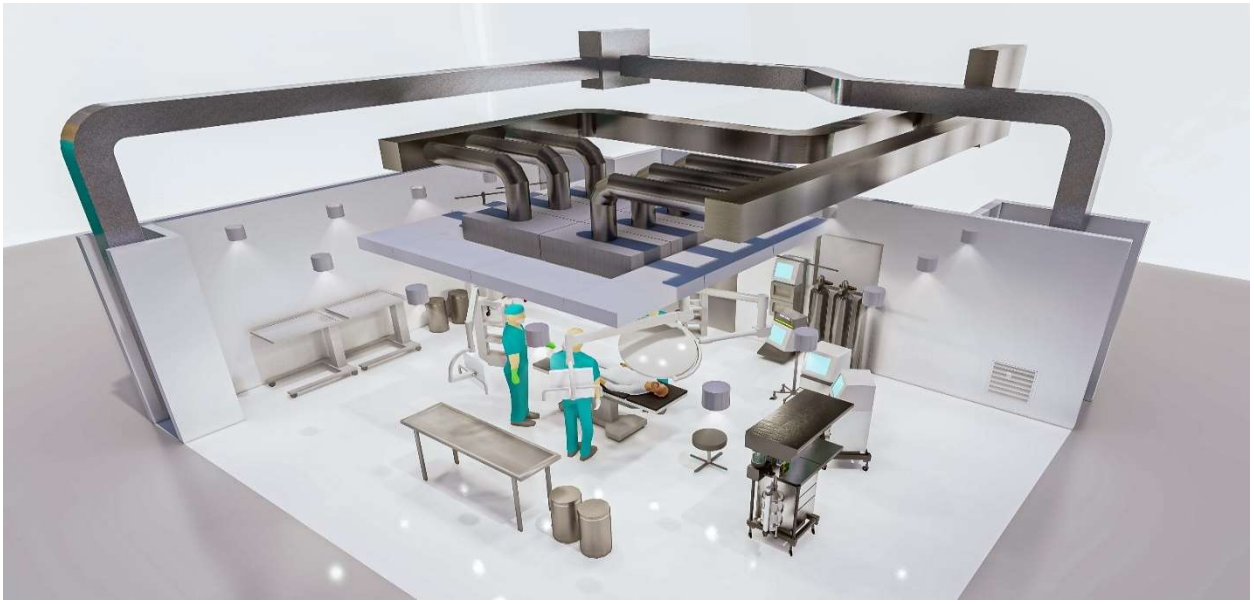

Figure 1: Operating Room, Clarksville, Texas

Figure 2 shows the proposed HVAC system for this OR comprises a chilled water coil Rooftop Unit (RTU) associated with an electric heating coil Variable Air Volume (VAV) system. Following ASHRAE 170-2017 design guidelines for the ventilation of surgery rooms, the use of laminal flow diffusers has been implemented to optimize the airflow pattern, ensuring precise distribution over both the patient and the surgical team. In addition, the inclusion of two strategically positioned low sidewall return air grilles at opposite corners facilitates efficient air circulation and effective containment and removal of contaminants.

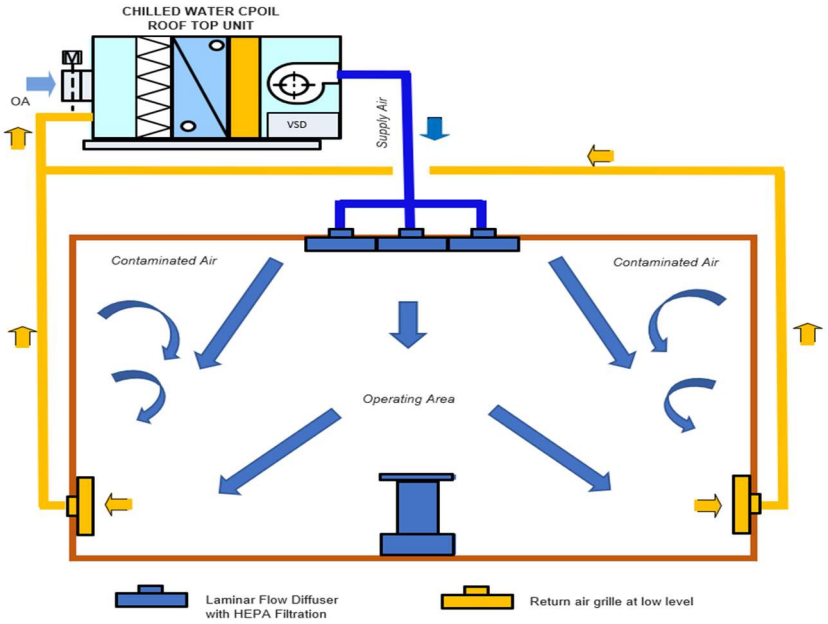

Figure 2- HVAC design schematic for operation room.

In accordance with ANSI/ASHRAE/ASHE Standard 170-2017 and TAC Title 25, Chapter 133, which establish the minimum HVAC design requirements for operating room ventilation systems, the ventilation system design criteria for this study are presented in Table 1. The total supply air volume is set at 23 air changes per hour (ACH), with the outdoor air change set at 4 ACH. The total return air flow rate, channeled through the two low sidewall return air grilles, is set to be lower than the total air flow rate from the laminal flow diffusers. This configuration ensures that the operating room (OR) consistently maintains a positive pressure relative to all adjacent spaces.

Design Requirement per ASHRAE 170 & TAC Title 25, Chapter 133	
Pressure	Positive
Air change per Hour	23
Out Door air change per Hour	4
Temperature Range (F)	68-75
Humidity Range	20-60
Noise Level (NC)	20-30
Class Filter MERV	7 & HEPA

Table 1 - Design required per ASHRAE 170 & TAC Title 25, Chapter 133

The design anticipates that the air flow pattern, utilizing laminal flow diffusers along with two low side walls return air grilles, can enclose the non-sterile zone. This setup prevents the intrusion of non-sterile air into the sterile area. The off-coil air temperature of the RTU is designed at 49.2 °F to keep the operating room's temperature within the desired range of 68 to 75°F. The humidity level is set at 44%. Additionally, the design of the chilled water coil RTU and its associated ductwork aims to keep the noise level between 20 to 30 dBA.

Results and Discussion

Velocity Pattern

The air exiting the laminal flow diffusers with HEPA filtration shapes the air column within the sterile zone, descending past the operating table before reaching the return air grilles. Essentially, the high-velocity discharge air from the supply air diffuser creates an air curtain that delineates the main sterile zone from the non-sterile zone, as illustrated in **Figure 3**. The laminar flow diffusers array covers an area extending more than 12 inches beyond each side of the surgical table's footprint, meeting the design criteria specified in ASHRAE 170 - 2017. The air velocity directly at the two return air grilles is notably higher, attributed to their considerably smaller surface areas in comparison to the laminal flow diffusers.

Concerning the velocity pattern, the findings indicate that the flow rate and external static pressure of the designed RTUs, the 23 selected total supply air change with 4 air change of outdoor air, in conjunction with the associated duct layout, have successfully met the prescribed design criteria outlined in ASHREA 170 and TAC. This configuration establishes an effective air barrier around the operating table, preventing contaminated air from the non-sterile zone from infiltrating into the sterile zone.

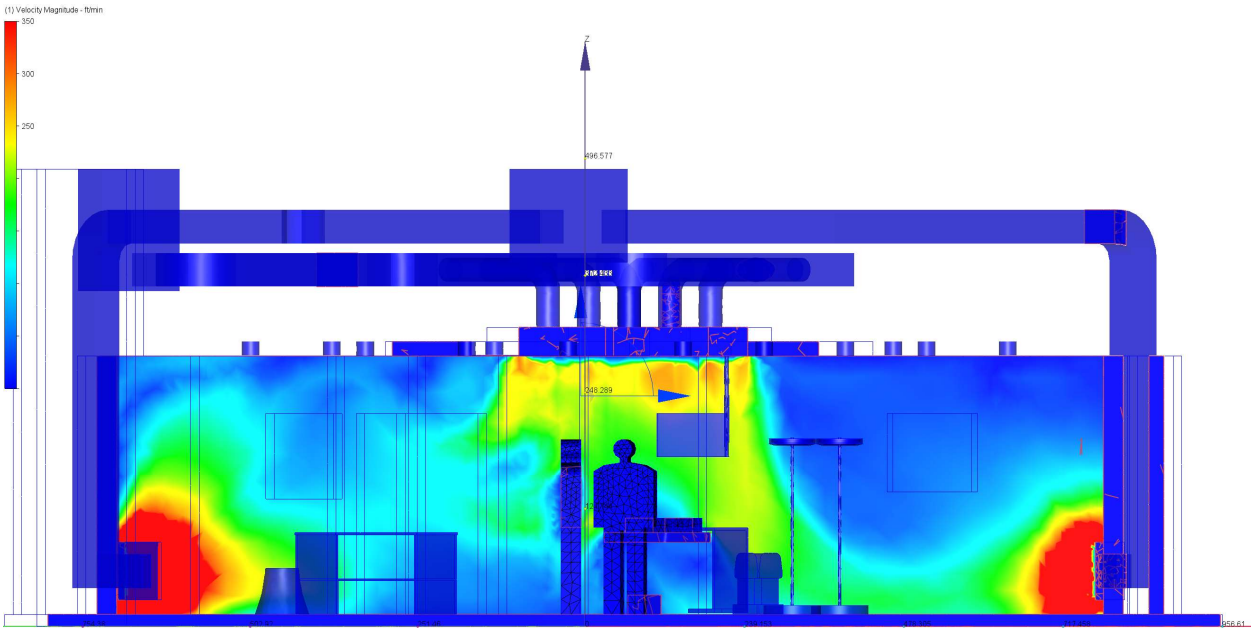

Figure 3a - The velocity distribution – Section View

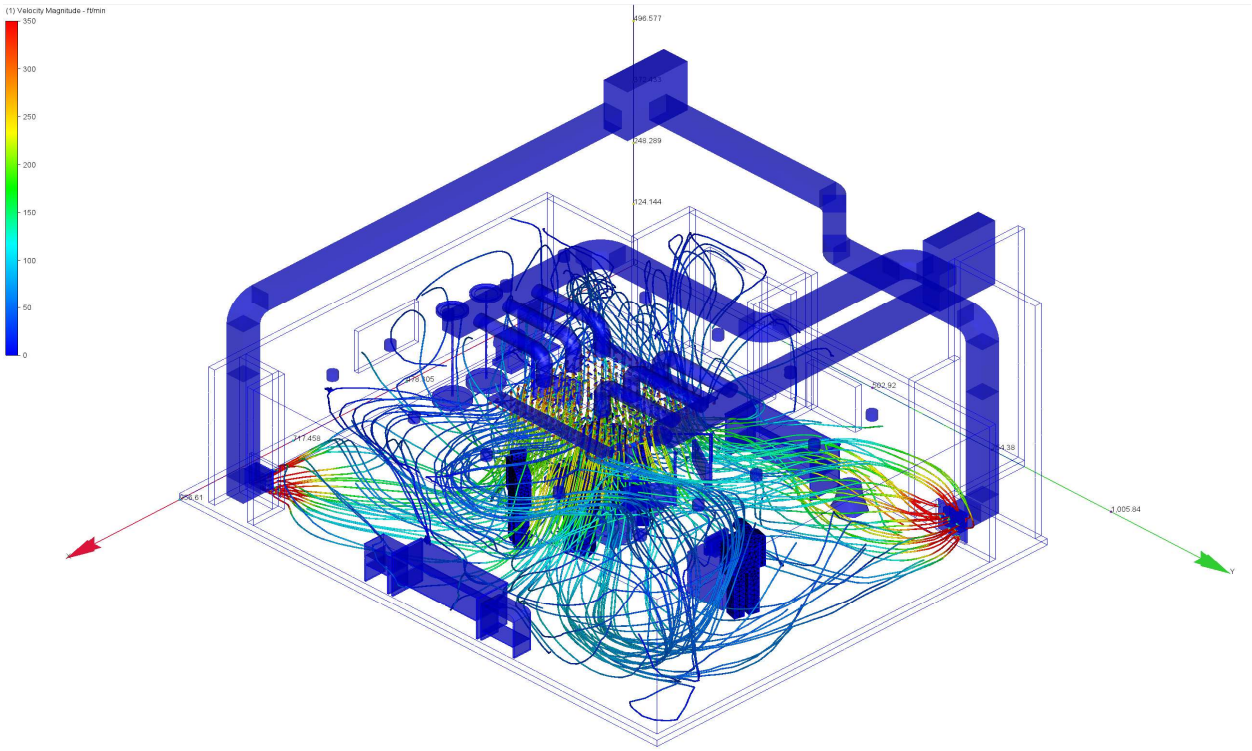

Figure 3b - The velocity distribution - Isometric View

Temperature Distribution

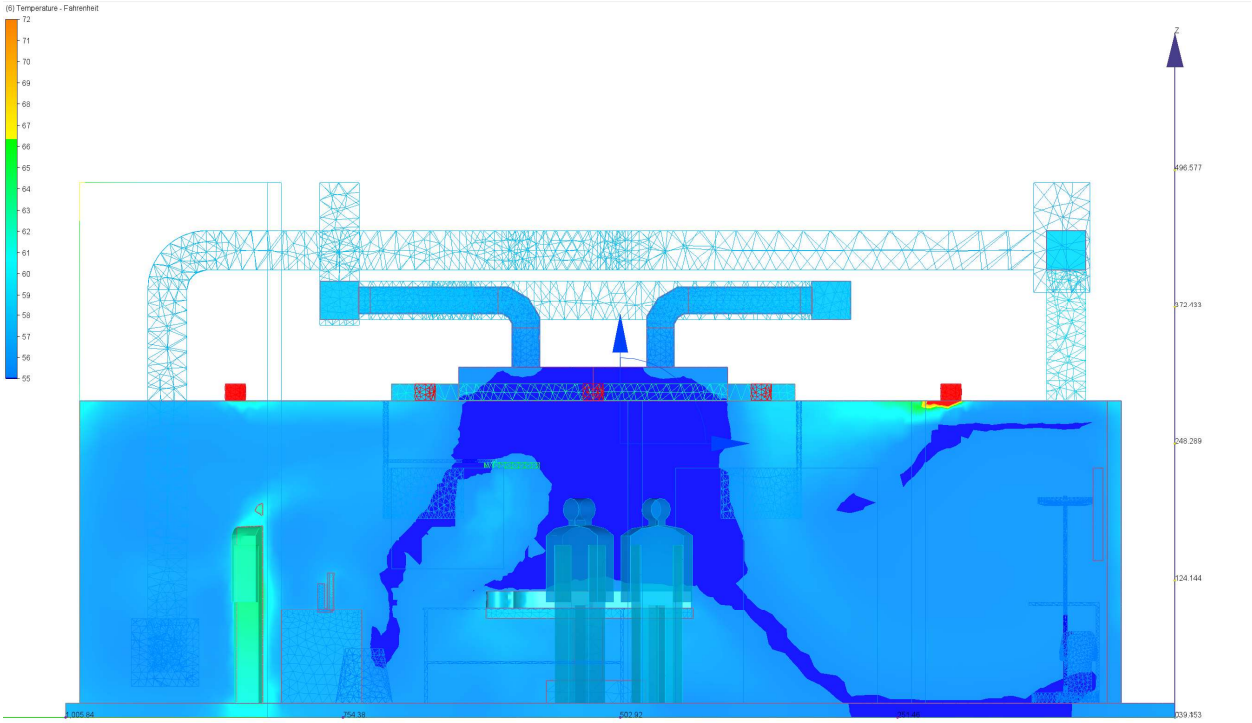

Figure 4a - The temperature distribution – Section View

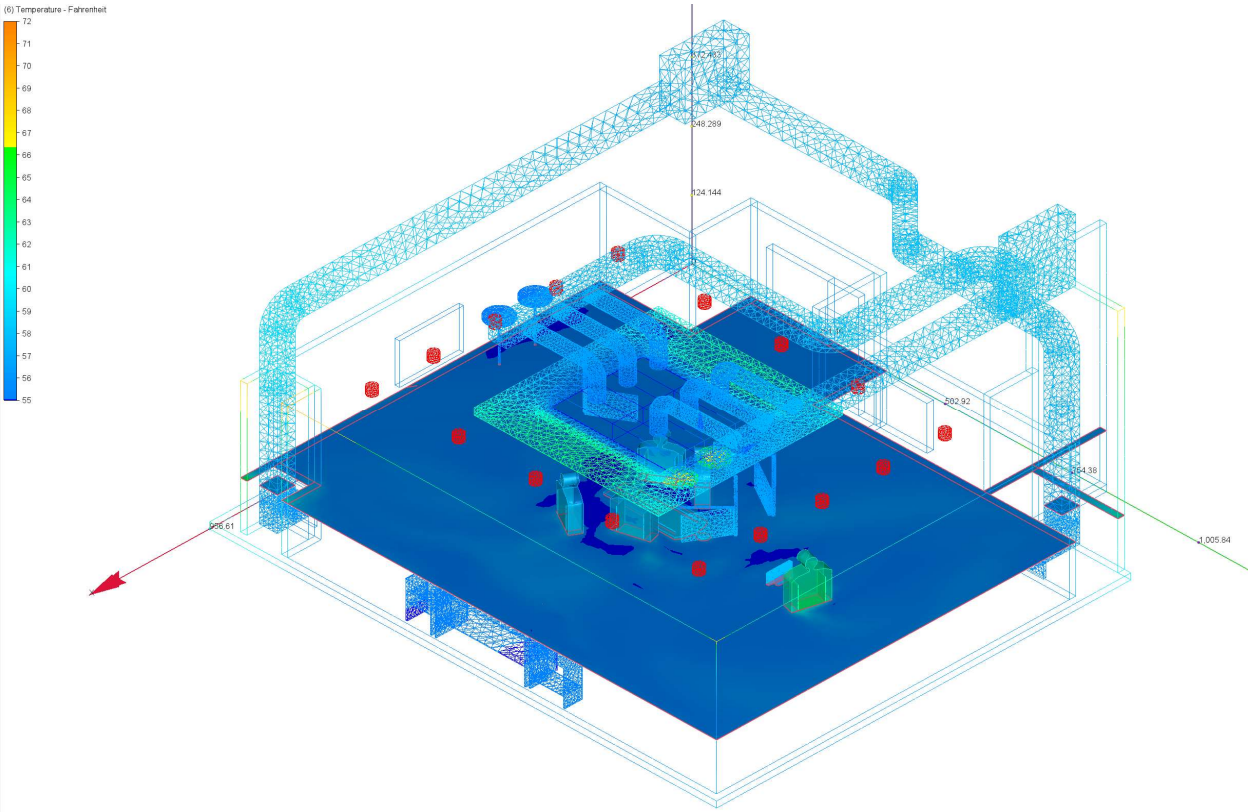

Figure 4b - The temperature distribution - Isometric View

The temperature distribution patterns, as illustrated in Figure 4, indicate a slight thermal rise between the sterile and non-sterile zones. Cold supply air from the laminal flow diffuser is entrained into the main core of the sterile zone, effectively lowering temperatures around the central core. The sterile zone temperatures are colder, ranging from 55 to 57 °F in contrast to the 58 to 61 °F observed in the non-sterile zone. Both temperature ranges are deemed suitable for the operating room (OR) environment, where heat rejections from medical equipment and operating lighting are prevalent

The average temperature in the non-critical zone is maintained at 61 °F. The lower temperature in the non-sterile zone contributes to enhanced thermal comfort for surgeons and nurses working in the OR, without any indications of accumulated hot air except for around the ceiling lighting fixtures and operating lights.

Considering the above results regarding the OR's temperature, it is evident that the overall temperature in the OR falls below the recommended range of 68 to 75 °F. While these lower temperatures may foster a thermally comfortable environment for most occupants, it is still recommended to adjust the off-coil temperature of the Rooftop Unit (RTU) to exceed the selected 49.2 °F for optimal HVAC system performance and efficiency.

Room Humidity Distribution

Designing the ventilation system for the operating room (OR) involves a unique requirement: maintaining the right room humidity. This element is essential for various reasons, including infection control, the well-being of patients and staff, optimal equipment performance, prevention of electrostatic discharge, support for optimal wound healing, and adherence to regulatory standards. The careful

management of humidity is important in establishing a safe, efficient, and comfortable environment for medical procedures. In accordance with ASHRAE 170 and TAC guidelines, the recommended humidity level in the OR should be maintained between 20% and 60% relative humidity (RH).

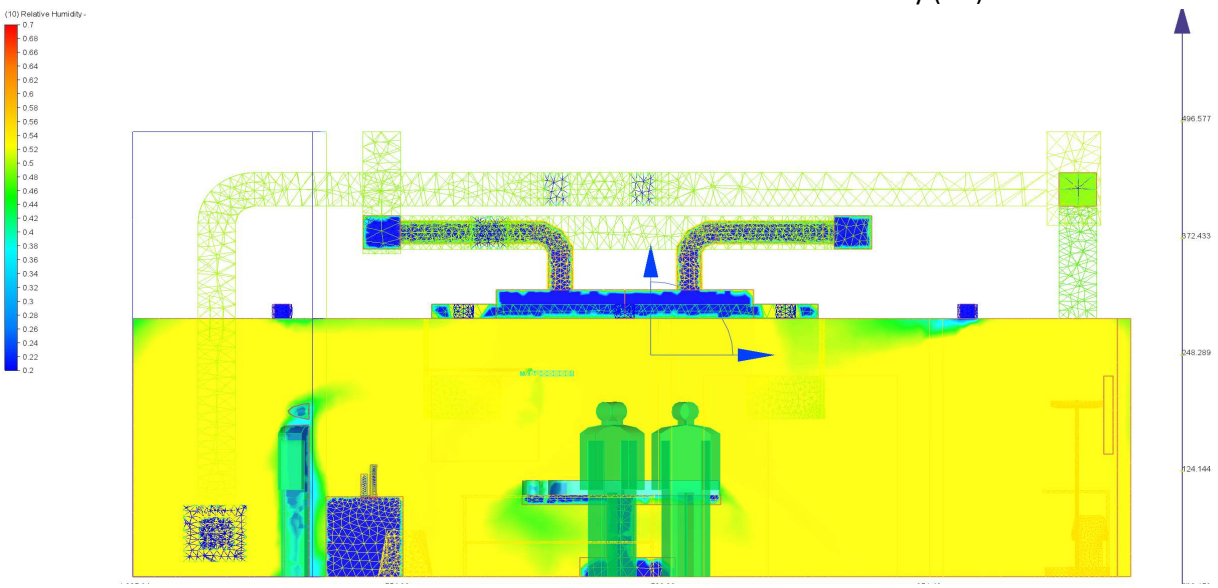

Figure 5a - The relative humidity distribution – Section View

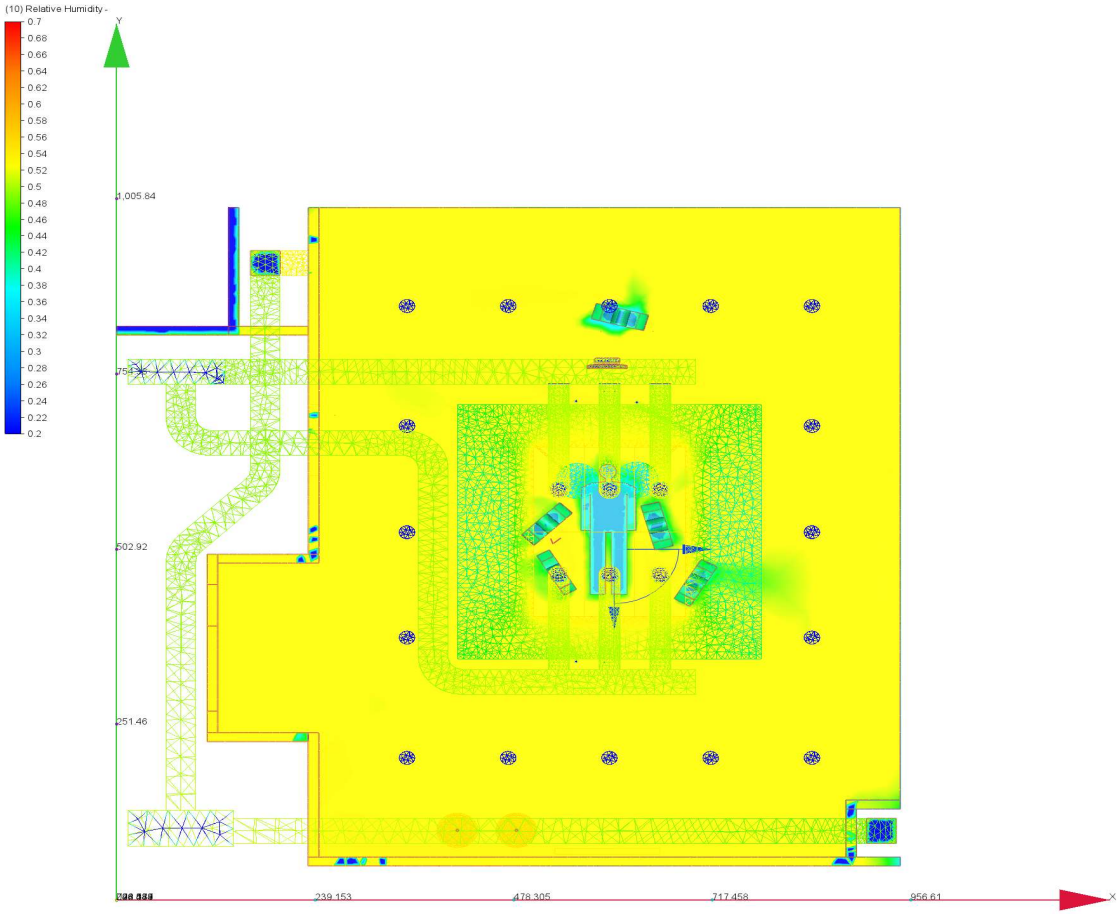

Figure 5b - The relative humidity distribution– Plan View

The findings, as illustrated in **Figure 5**, reveal the humidity pattern in the OR. In the sterile zone, humidity ranges from 48% to 55%, while in the non-critical zone, it ranges from 48% to 51%. The slightly higher humidity in the sterile zone is a result of introducing 4 air changes of outside air, which is blended with the return air in the RTUs. After leaving the sterile zone, the humidity level shows a gradient since there are no sources of latent heat except for the occupants within the room. On average, the humidity in the operating room is 52%, aligning with the design requirements outlined by both ASHRAE and TAC (20% to 60%).

In conclusion, the simulation results for temperature, humidity, and velocity distribution reveal that, with the exception of the overall temperature in the OR falling below the recommended range – an issue addressable by increasing the off-coil temperature of the Rooftop Unit (RTU) – the existing HVAC system design for the operating room effectively meets the design standards outlined by ASHRAE 170 and TAC.

Case Study 3

Designing Ventilation Systems for Underground Parking Garage

Woodinville, Washington

The basement car park presents distinctive challenges due to its enclosed nature, limited natural ventilation, and the potential introduction of pollutants from vehicle exhausts. Efficient ventilation plays a critical role not only in maintaining air quality but also in addressing fire hazards and ensuring thermal comfort. ASHRAE 62.1 has established specific requirements for air quality in enclosed parking facilities, measured in air changes per hour (ACH). The recommended values are a minimum of 6 ACH for normal operation and 9 ACH for fire mode. In addition, the 2018 International Mechanical Code (IMC), section 404.1 Enclosed Parking Garages specifies air quality requirements for ventilation in enclosed parking garages, equivalent to 0.75 CFM/SF.

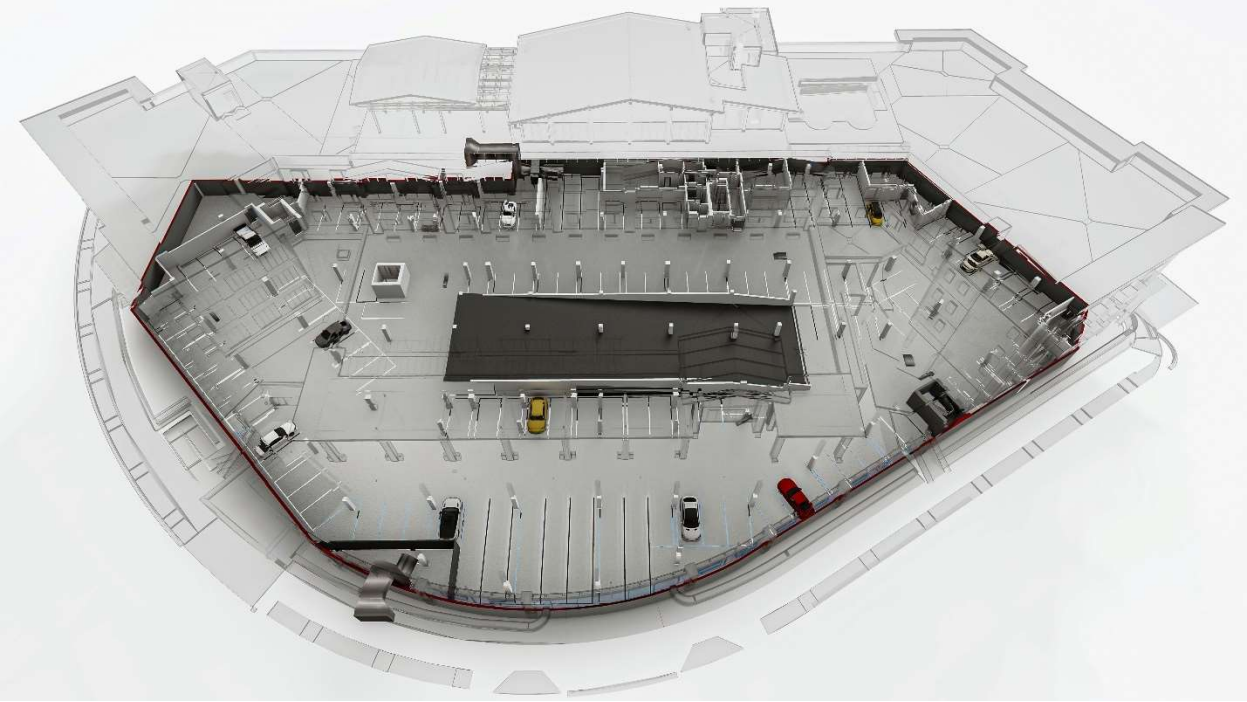

Figure 1: Enclosed Parking Garage located in basement Level P2

In this study, we employ Computational Fluid Dynamics (CFD) simulations to investigate air flow velocities and Local Mean Age (LMA) in normal mode for the initial ventilation design. We consider three different configurations of ventilation systems for a 60,998-square-foot enclosed parking garage (P2) situated in a 2-basement and 5-story hotel located in Woodinville, Washington State, the initial design specifies a ventilation rate of 0.75 CFM/SF for the ventilation fans during normal operation. Our study aims to achieve the required LMA values at the 1.7-meter level within the basement car park, adhering to a stringent threshold of less than 15 minutes. The emphasis on LMA is crucial, as it represents one of the most essential parameters when assessing contaminant removal or evaluating ventilation efficiency

in enclosed spaces, as highlighted by Liddament (1993). This study outlines three configurations of ventilation systems in the initial design as follows:

Option 1: In this configuration, parking garage 2 (P2) is ventilated with only one exhaust air fan with a total flow rate of 45,000 CFM and ESP of 0.5 in wg is located on the south side of Parking Garage 2. It is assumed that outside air will enter through the ram passing through Parking Garage P1 and Parking Garage P2. The airflow diagram is illustrated in **Figure 2**

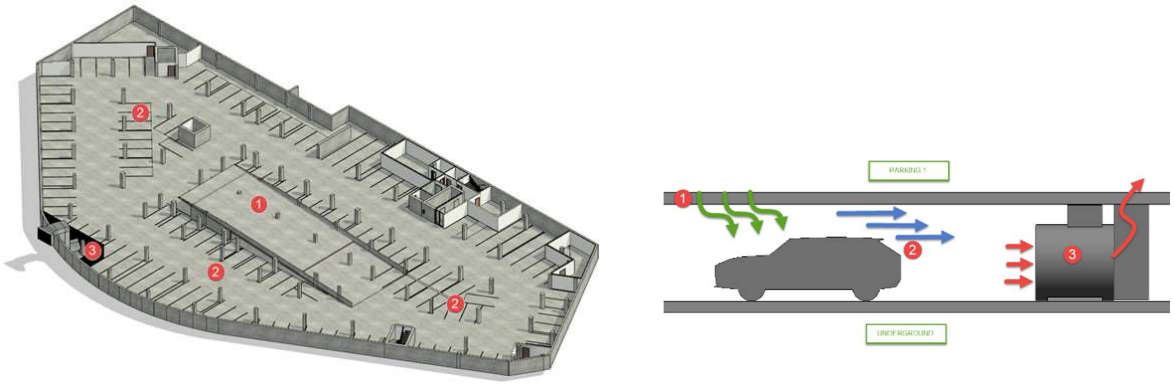

Figure 2: Parking Garage Ventilation Concept - Featuring a Single Exhaust Fan

Notes:

1. *Air intake for makeup air sourced from/to Parking Level P1.*
2. *Pathway for exhaust air leading to the garage exhaust fan.*
3. *Discharge from the garage exhaust fan directed to the exterior wall at Level 1.*

Option 2: In this configuration, alongside the exhaust air fan, we incorporate two jet fans, each with a capacity of 5,500 CFM, positioned on the north and east sides of Parking Garage 2. The inclusion of two jet fans serves the purpose of expediting air transfer to the exhaust air fan. The airflow diagram is depicted in **Figure 3**

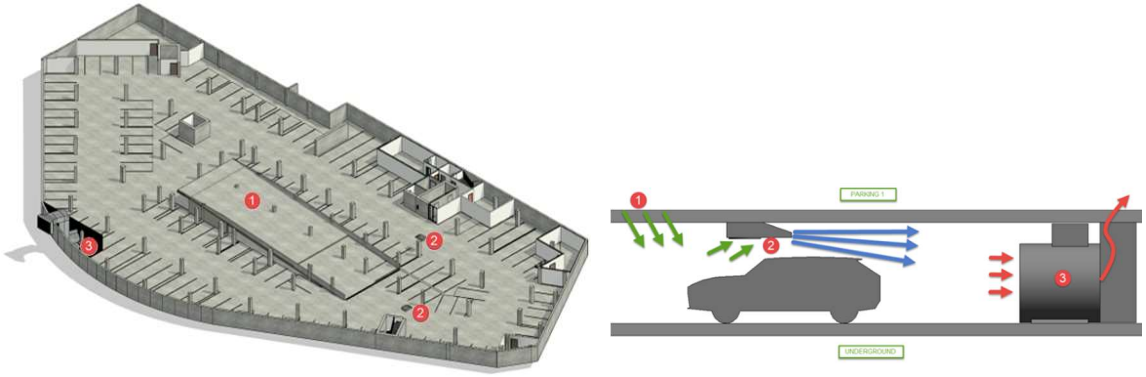

Figure 3: Parking Garage Ventilation Concept - Incorporating One Exhaust Fan and Two Jet Fans

Notes:

1. *Air intake for makeup air sourced from/to Parking Level P1.*
2. *Two jet fans facilitate air distribution within the parking garage.*

3. *Discharge from the garage exhaust fan directed to the exterior wall at Level 1.*

Option 3: In this configuration, the ventilation system for Parking Garage P2 comprises one exhaust air fan at 45,000 CFM with 0.5 in wg, one makeup air fan at 45,000 CFM with 0.5 wg, and seven axial jet fans, each rated at 6,010 CFM. The makeup air fan is situated on the north side of the parking garage P2, drawing fresh air through a chase and external louvre at level P1. The exhaust air fan is located on the south side of P2. Ductless jet air fans are strategically distributed throughout P2 to enhance and transfer air from the north to the south. The airflow diagram is presented in **Figure 4.**

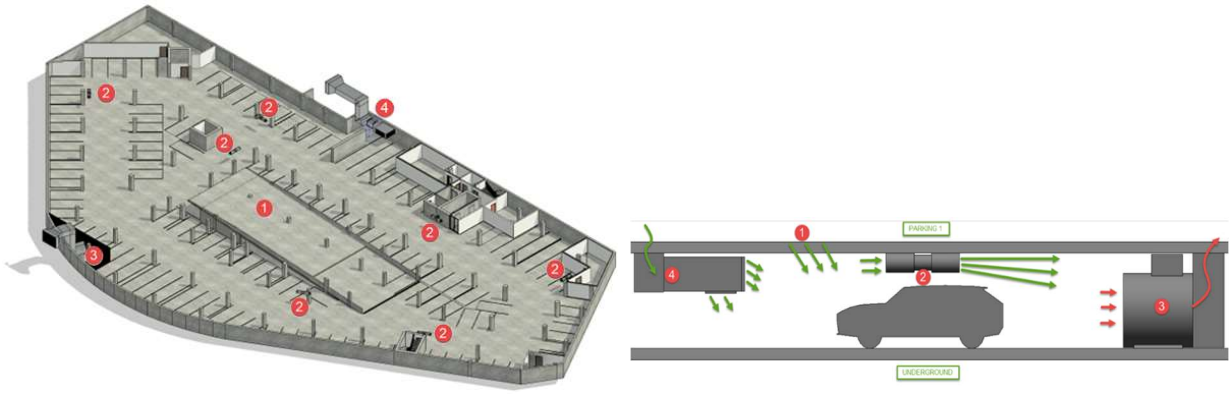

Figure 4: Parking Garage Ventilation Concept - Incorporating One Exhaust Fan, One Makeup Fan and Seven Jet Fans

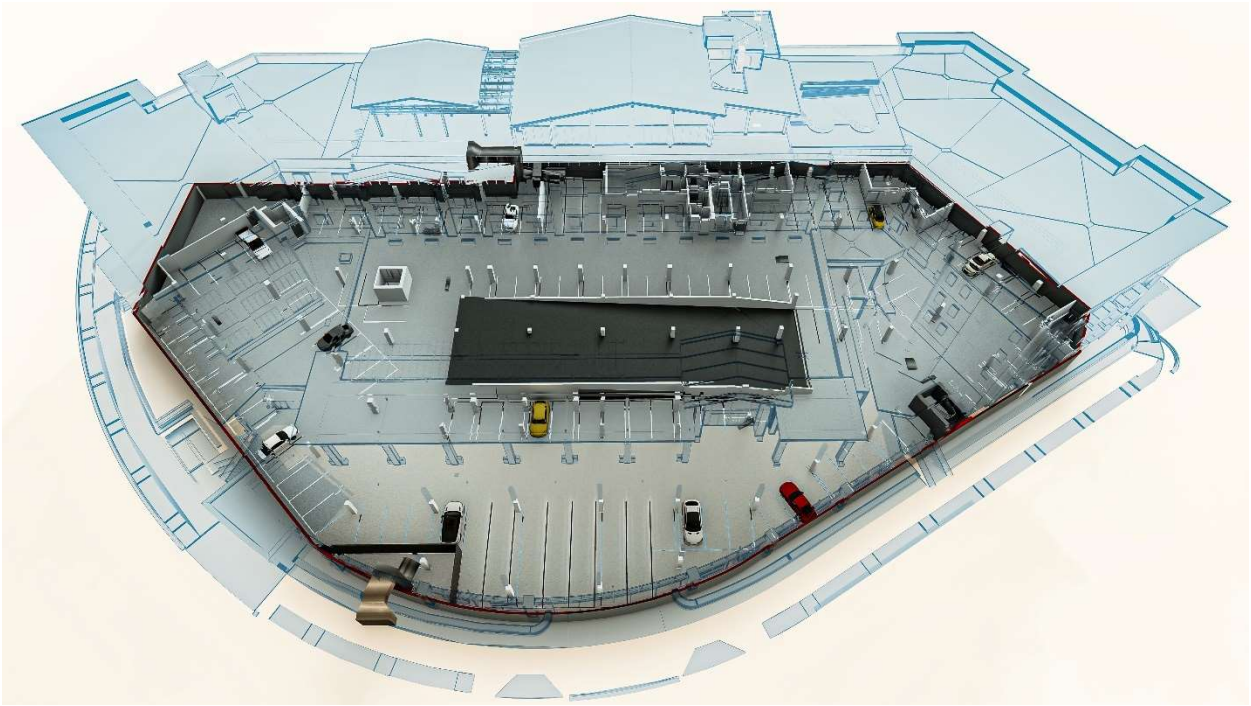

Notes:

1. *Air intake for makeup air sourced from/to Parking Level P1*

2. *Seven jet fans facilitate air distribution within the parking garage.*
3. *Discharge from the garage exhaust fan directed to the exterior wall at Level 1*
4. *Makeup air fan.*

Results and Discussion

LMA and Velocity Distributions for Initial Design

Figure 1 and **Figure 2** illustrate the distribution of velocity and LMA at the 1.7m plan level for all three options of initial design.

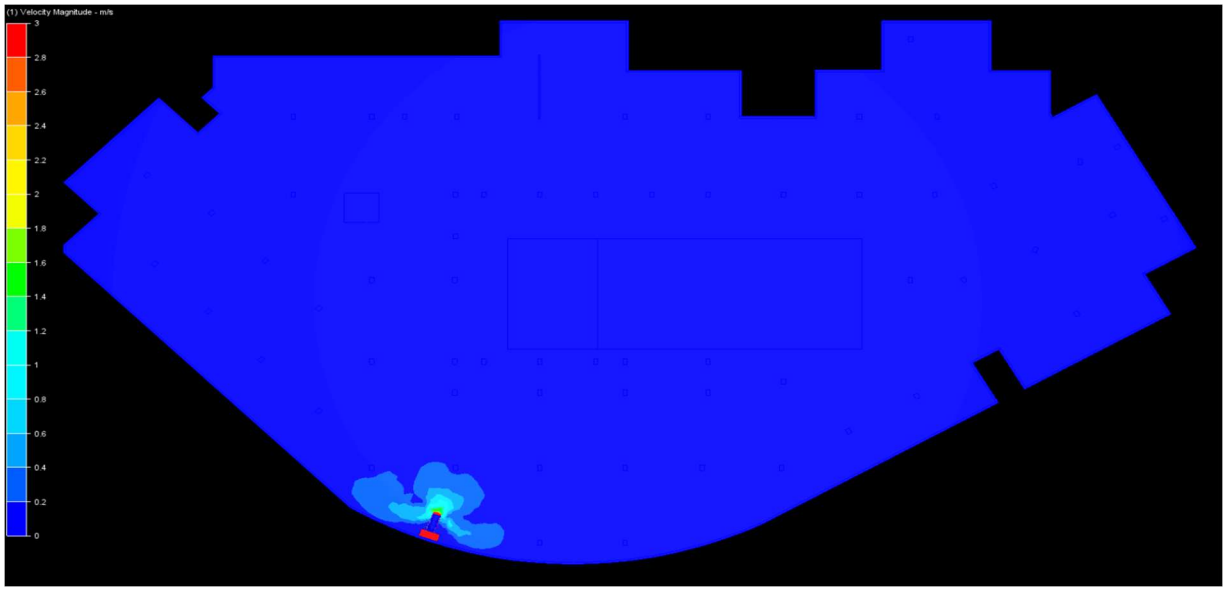

Fig. 1a: Velocity Distribution at the 1.7m Plan Level for Option 1 - One Exhaust Fan

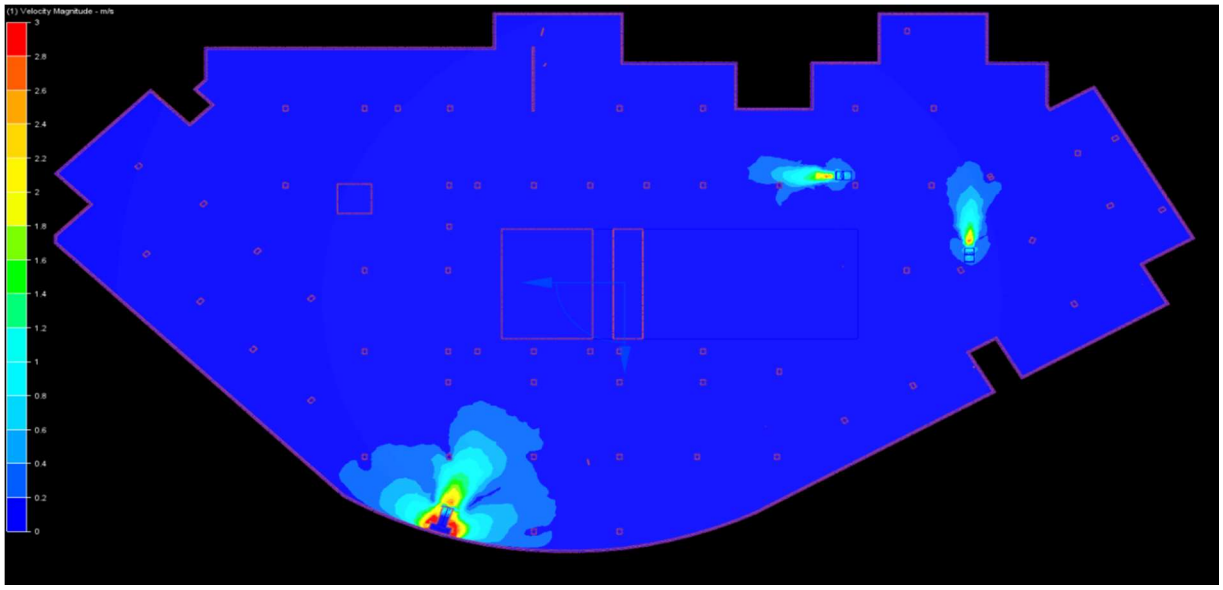

Fig. 1b: Velocity Distribution at the 1.7m Plan Level for Option 2 - One exhaust Fan, 2 jet fans

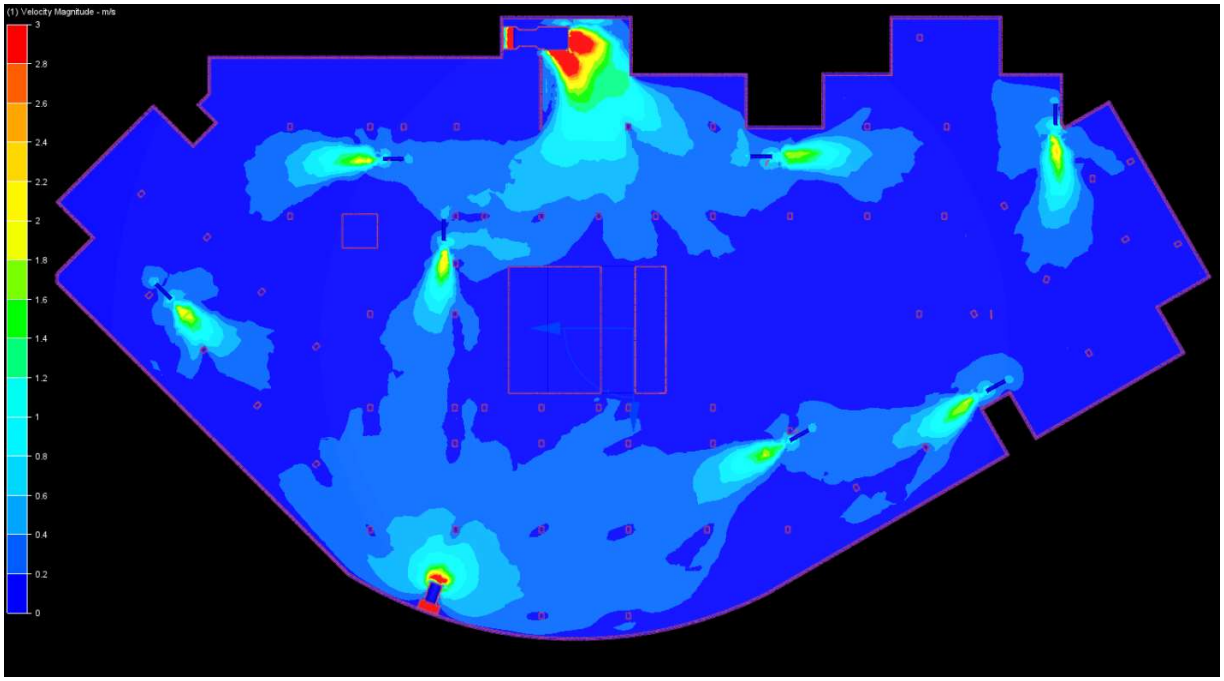

Fig. 1c: Velocity Distribution at the 1.7m Plan Level for Option 3 - One exhaust Fan, 7 jet fans, and one makeup fan.

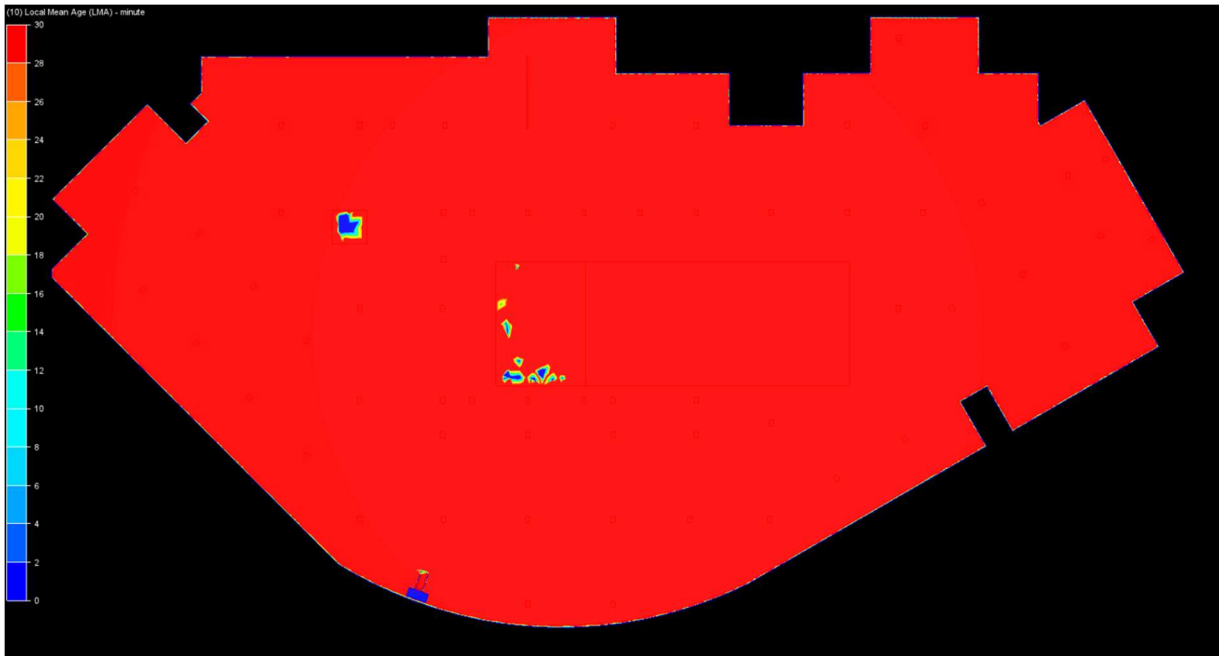

Fig. 2a: LMA Distribution at the 1.7m Plan Level for Option 1 - One Exhaust Fan

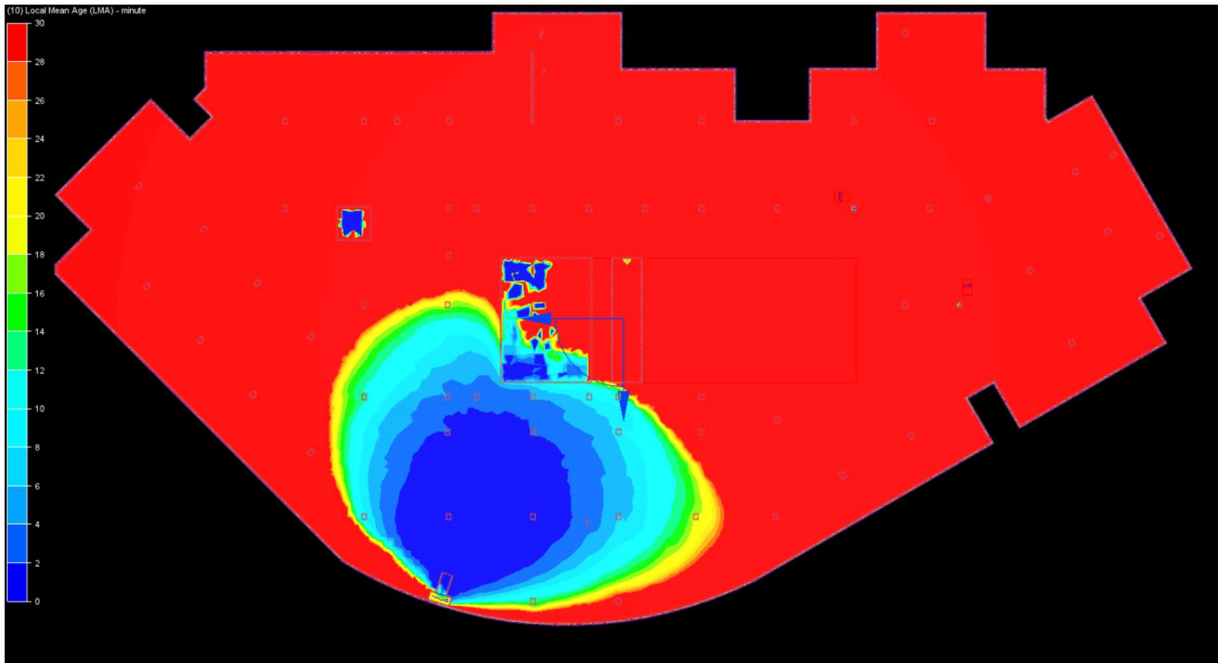

Fig. 2b: LMA Distribution at the 1.7m Plan Level for Option 2 - One exhaust Fan, 2 jet fans

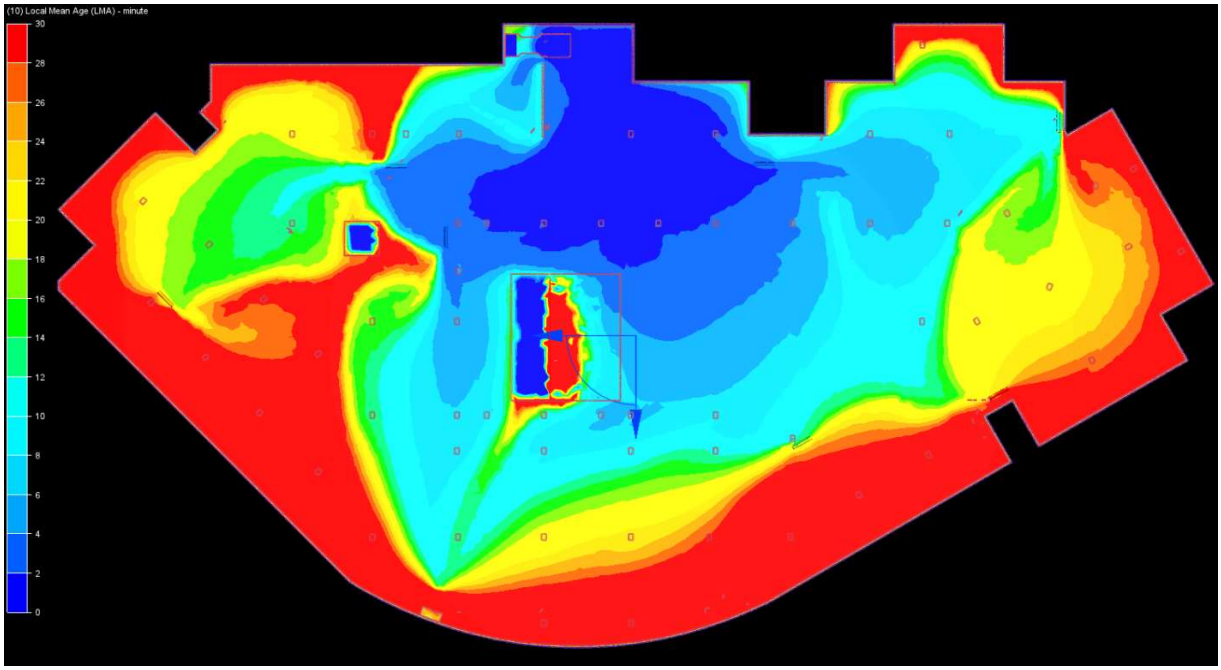

Fig. 2c: LMA Distribution at the 1.7m Plan Level for Option 3 - One exhaust Fan, 7 jet fans, and one makeup fan.

It is evident from the simulation results that none of the options proposed in the initial design meet the specified design criteria for both velocity and LMA (Local Mean Age) values. Examining the velocity pattern, both Option 1 and Option 2 exhibit almost zero velocity, indicated by a dark blue coloration in the simulation results, suggesting the presence of dead zones or significant air stagnation. The additional 2 jet fans in Option 2 does not have any positive effect in velocity.

Despite the inclusion of a makeup air fan and an additional seven jet fans to direct the air stream, the velocity pattern of Option 3 shows improvement, with the average velocities ranging from 0.2 m/s to 0.6 m/s. However, it appears that over 80% of the areas still experience dead zones, indicating a substantial failure to meet the design criteria for basement car park ventilation.

The velocity pattern simulation results align consistently with those obtained from the LMA. For Option 1, Option 2, and Option 3, more than 90%, 80%, and 70% of the LMA-covered area exceeds 15', respectively. Option 1 and Option 2 are identified as nearly dark zones with exceptionally high LMA values greater than 30 minutes. In the case of Option 3, containing makeup air and seven jet fans, the air contours reveal stagnation and recirculation in various sections of the basement car park. This observation prompts considerations for enhancing LMA distribution, suggesting potential improvements through increasing air change, adjustments to jet fan locations, capacities, flow angles, as well as changes to the positions of main supply air grilles and exhaust air grilles.

The simulation outcomes for both LMA and velocity indicate that none of the initially proposed options meet the required design standards adequately. As a result, alternative approaches have been proposed, involving increased fan capacities for both makeup and exhaust air fans, relocating and adjustment of flow angles for jet fans. Furthermore, the repositioning of the main supply and exhaust air grilles is considered to enhance air distribution throughout the entire car park area. The summarized details of the new proposed options are presented below:

Option 4: Based on 6 air changes, supply/exhaust air fans at 55,000 CFM, 7 jet fans at 6,010 CFM, maintaining the same fan room/ductwork layout as the initial design.

Option 5: Based on 9 air changes, supply/exhaust air fans at 82,400 CFM, 7 jet fans at 6,010 CFM, maintaining the same fan room/ductwork layout as the initial design.

Option 6: Based on 6 air changes, supply/exhaust air fans at 55,000 CFM, 7 jet fans at 6,010 CFM, involving the relocation of fan rooms in carpark 1 to change the locations of main supply/exhaust air grilles in carpark 2. It also includes relocating jet fan locations and adjusting flow angles to address stagnation and recirculation areas, as illustrated in Figure 3.

Option 7: Based on 9 air changes, supply/exhaust air fans at 82,400 CFM, 7 jet fans at 6,010 CFM, involving the relocation of fan rooms in carpark 1 to change the locations of main supply/exhaust air grilles in carpark 2. This option also includes relocating jet fan locations and adjusting flow angles to address stagnation and recirculation areas, as shown in **Figure 3.**

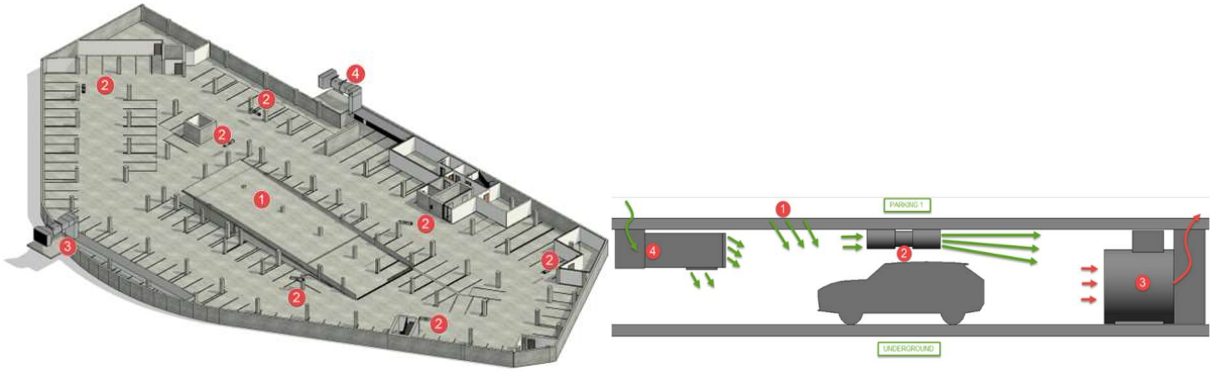

Figure 3. Revised ductwork layout and main supply/exhaust air grilles relocation for the parking garage

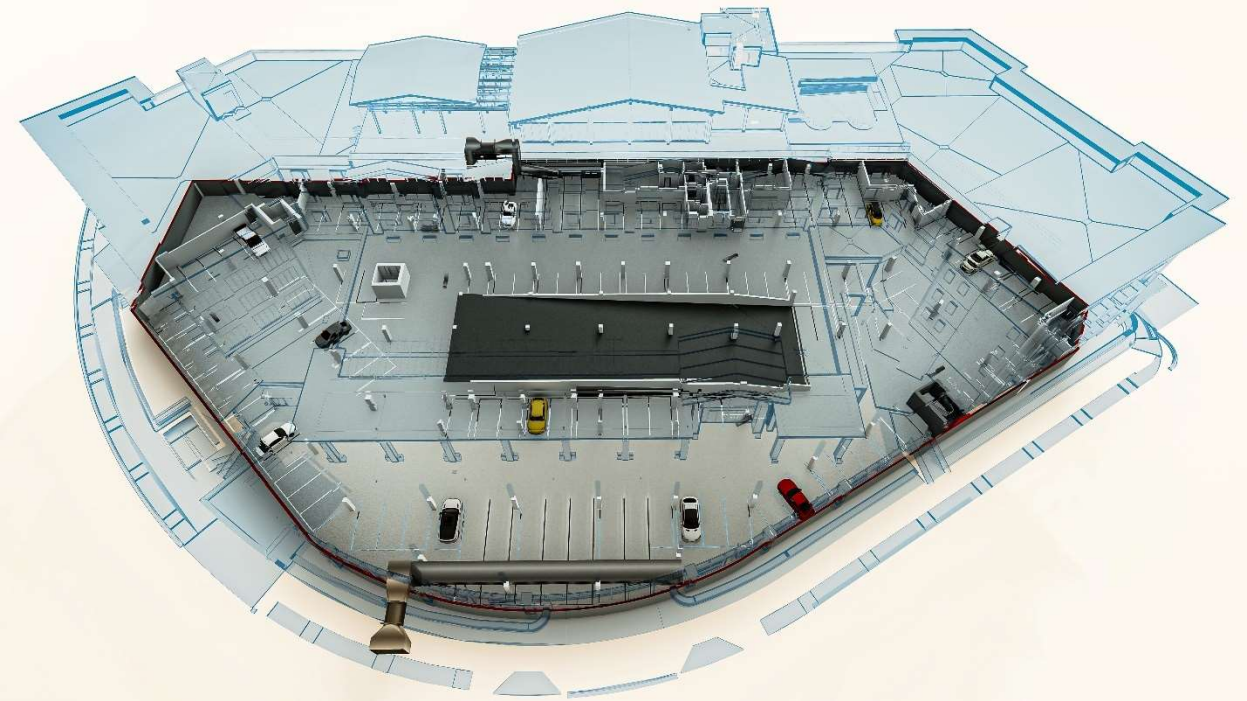

Notes:

1. *Air intake for makeup air sourced from/to Parking Level P1*
2. *Seven jet fans facilitate air distribution within the parking garage.*
3. *Discharge from the garage exhaust fan directed to the exterior wall at Level 1*
4. *Makeup air fan.*

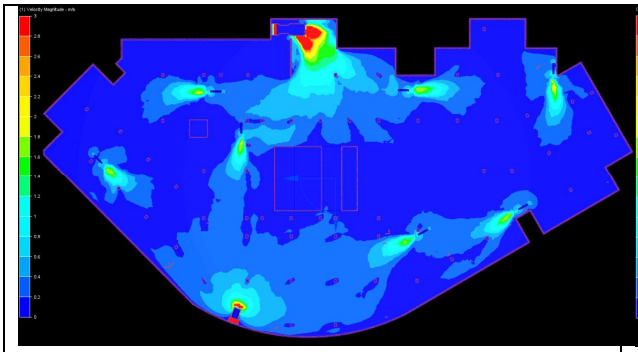

***Fig. 4a**: Velocity distribution at the 1.7m plan level for Option 4 - 6 ACH*

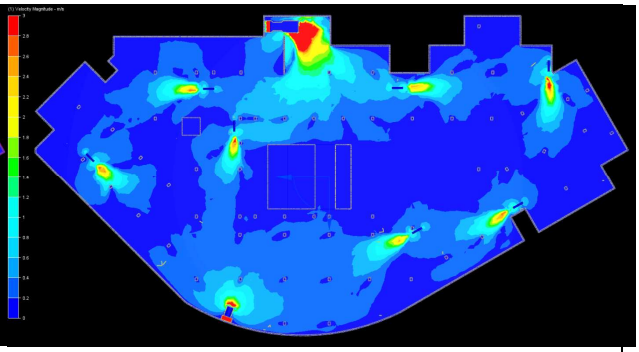

***Fig. 4b**: Velocity distribution at the 1.7m plan level for Option 5 - 9 ACH*

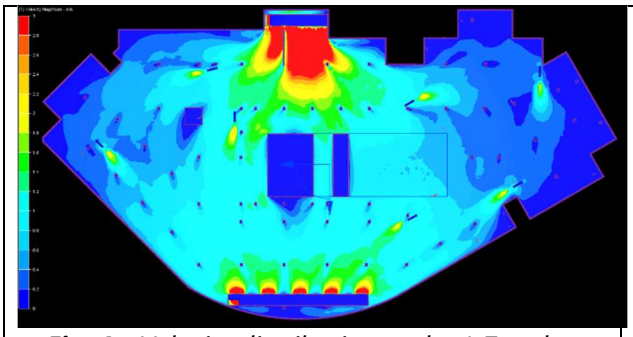

***Fig. 4c**: Velocity distribution at the 1.7m plan level for Option # 6 - 6 ACH*

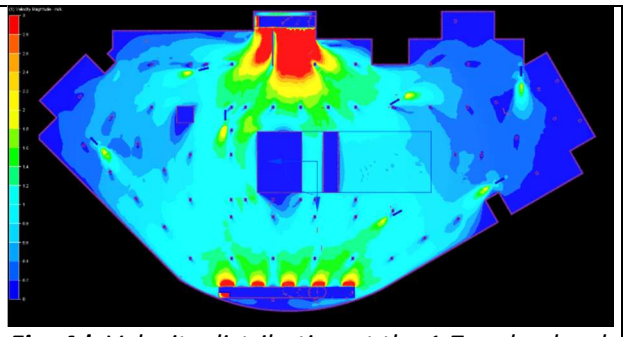

***Fig. 4d**: Velocity distribution at the 1.7m plan level for Option # 7 - 9 ACH*

Figure 4: Velocity Distributions at the 1.7m plan level for Option 4, Option 5, Option 6, and Option 7

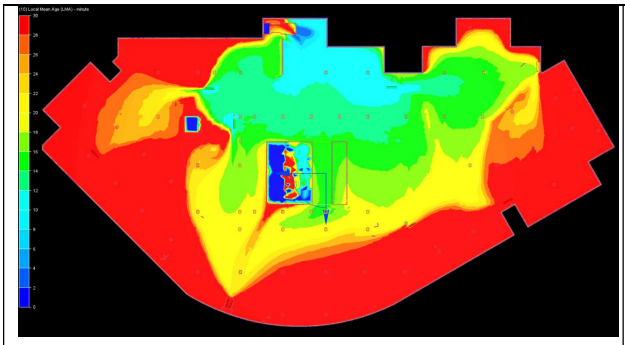

***Fig. 5a**: LMA distribution at the 1.7m Plan Level for Option 4 - 6 ACH*

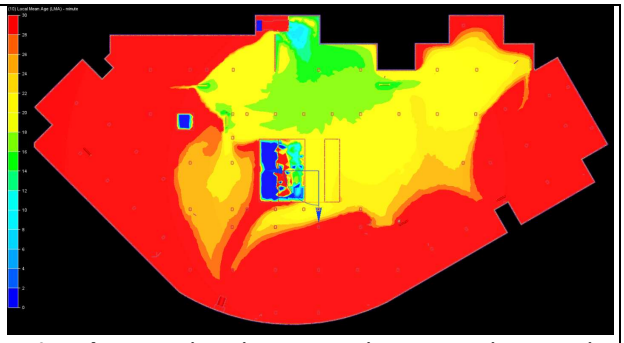

***Fig. 5b**: LMA distribution at the 1.7m Plan Level for Option 5 - 9 ACH*

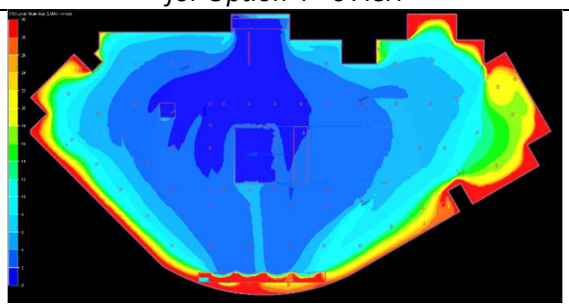

***Fig. 5c**: LMA distribution at the 1.7m Plan Level for Option 6 - 6 ACH*

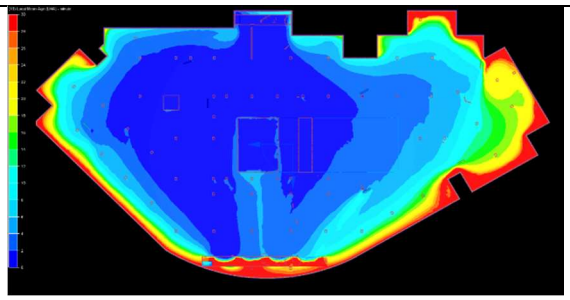

***Fig. 5d**: LMA distribution at the 1.7m Plan Level for Option #7 - 9 ACH*

Figure 5: LMA Distributions at the 1.7m plan level for Option 4, Option5, Option 6, and Option 7

The simulation result for the 4 above options for both velocity and LMA distributions are shown in **Figure 4** and **Figure 5**, respectively. The simulation results indicate that, when maintaining the same ductwork layout as the initial design, the increase in the capacity of makeup and supply air fans (based on 0.75 CFM/SF in the initial design to 6 or 9 air changes for option 4 and 5, respectively) do not gain significantly positive changes in both velocity and LMA air distribution. Under Option 4 (4 air changes), over 85% of the car park area experiences velocities ranging from 0 to 0.4m/s. Option 5 (5 air changes) shows slightly improved results, with velocities ranging from 0 to 0.4 m/s for over 80% of the carpark areas. The velocity simulation results align with LMA distribution, with nearly 80% of the car park area exhibiting LMA values significantly exceeding 15 minutes for both Option 4 and Option 5.

Moreover, the analysis of velocity distribution for both options indicates that the central section of the car park mostly experiences zero velocity. This observation prompts the consideration of Options 6

and 7, which result in relocating fan rooms to car park P1 to reposition the main supply/exhaust air grilles to a more central and wider configuration within car park 2. The proposed adjustments also involve relocating jet fan locations and adjusting flow angles to address stagnation and recirculation areas.

The simulation results clearly demonstrate that the repositioning of main supply/exhaust air grilles, along with the relocation of jet fan locations and adjustment of jet fan flow angles in both Option 6 and Option 7, successfully meet the design criteria for basement carpark ventilation. In both options, the LMA for over 70% of the carpark areas is less than 15 minutes, while velocities exceed 1m/s for more than 70% of the carpark area.

Option 7 shows a slightly superior performance in LMA distribution, with 86.92% of the total car park area achieving an LMA of less than 15 minutes, compared to 78.93% in Option 6. However, considering cost considerations, Option 6 is recommended. The summarized results of LMA for all four options are presented in Table 2.

LMA Table Analysis								
	Option 4: 6ACH		Option 5: 9ACH		Option 6: 6ACH		Option 7: 9ACH	
	41.97%	41.97%	47.69%	47.69%	35.54%	35.54%	39.10%	39.1%
	9.82%	9.82%	11.45%	11.45%	15.53%	15.53%	16.82%	16.82%
	8.64%	8.64%	10.99%	10.99%	8.95%	8.95%	9.81%	9.81%
	7.30%	7.3%	8.51%	8.51%	6.94%	6.94%	7.35%	7.35%
	5.77%	5.77%	7.17%	7.17%	5.23%	5.23%	6.67%	6.67%
	5.34%	5.34%	3.39%	3.39%	4.68%	4.68%	3.24%	3.24%
	4.85%	4.85%	3.14%	3.14%	4.30%	4.3%	3.22%	3.22%
	4.77%	4.77%	1.92%	1.92%	4.03%	4.03%	2.97%	2.97%
	3.72%	3.72%	1.56%	1.56%	3.89%	3.89%	2.93%	2.93%
	3.03%	3.03%	1.40%	1.4%	3.26%	3.26%	2.48%	2.48%
	2.86%	2.86%	0.62%	0.62%	2.97%	2.97%	1.47%	1.47%
	1.12%	1.12%	0.60%	0.6%	1.62%	1.62%	1.44%	1.44%
	0.47%	0.47%	0.54%	0.54%	0.93%	0.93%	0.88%	0.88%
	0.33%	0.33%	0.36%	0.36%	0.85%	0.85%	0.82%	0.82%
	0.00%	<0%	0.35%	0.35%	0.84%	0.84%	0.45%	0.45%
	0.00%	<0%	0.30%	0.3%	0.42%	0.42%	0.35%	0.35%
Total % with no background color	53.25%		50.16%		61.42%		58.40%	
Sum LMA under 15 minutes	19.80%		6.10%		48.48%		50.76%	
LMA Percentge under 15 minute	37.18%		12.16%		78.93%		86.92%	

Table 2 LMA Table Analysis

Conclusion

In concluding our exploration of CFD applications for MEP systems, the underlined complexities shown in our real-world case studies highlight the vital role of CFD in addressing complex design challenges. The depth of our analyses reveals that CFD is not merely a tool but an effective method for achieving superior MEP system designs.

The first case study investigated a data center in San Juan, Puerto Rico, where thorough examination of the initial design for the HVAC system of the facility, through CFD simulations. These simulations provided a dynamic representation of air velocity, static pressure, humidity, and temperature distributions within the facility. Through this simulated exploration, the MEP engineers identified inefficiencies in the design, particularly focusing on the specifications of the CRAC units. One of the key findings was related to ESP and LAT parameters specified for the CRAC units, which were found to be inadequate. These parameters play a key role in determining the efficiency and effectiveness of the HVAC system designed for the data center. The CFD simulations facilitated precise adjustment of ESP and LAT values until the simulation outputs aligned with the strict design criteria established for the data center, particularly concerning the incoming and outgoing temperatures of server racks. Provided with valuable insights from the CFD simulation outputs, the MEP engineers carefully evaluated newly proposed options to select the optimal ESP and LAT values, ensuring optimal operation of the CRAC units in meeting the specified requirements for server rack temperatures.

Proceeding to the second case study, a detailed investigation studied the complexities of a hospital operating room located in Clarksville, Texas. Applying CFD analysis, a comprehensive analysis was conducted to validate the proposed HVAC system design. The outcomes of the CFD analysis served as a strong verification, confirming the HVAC system designed strictly comply with current healthcare codes and standards. The absence of CFD validation for the proposed HVAC system design presents a formidable challenge for the MEP engineer to ensure full compliance with critical design requirements. Numerous factors, including the layout of operating room furniture, the presence of operating equipment, and the number of occupants in the operating room, significantly influence HVAC system design. Moreover, considering the potential life-saving or life-threatening consequences of system failure in these critical settings, the risks are exceptionally high. This underscores the important role of CFD in simulating the proposed HVAC design. By employing CFD, the MEP engineer has the flexibility to dynamically modify design parameters as necessary, for example, raising the off-coil temperature of the Rooftop Unit (RTU). This adjustment ensures the design meets the strict requirements established by contemporary healthcare standards and design guidelines. The utilization of CFD not only enhances the precision of the HVAC system but also serves as a crucial tool in mitigating risks and ensuring the optimal functionality of the system in critical healthcare environments.

The third case study provides a detailed exposition on how the strategic application of CFD facilitates the MEP engineer in selecting the optimal configuration for the mechanical ventilation system within an underground car park, ensuring strict compliance to regulatory standards. Initially, the CFD analysis exposes deficiencies in all three initial options concerning the prescribed criteria for Local Mean Age (LMA) and velocity distributions. Upon a thorough examination of the simulation results to identify the root causes of these shortcomings, the MEP engineer gains insights into the system's dynamics. Provided with this comprehensive understanding, alternative design options are systematically proposed to rectify the identified deficiencies. The exploration ultimately leads to the discovery that optimizing airflow distribution involves strategic adjustments, including repositioning air grilles, modifying the

airflow angles of jet fans, reconfiguring ductwork, and increasing the capacity of make-up/exhaust air fans. The outcome of these detailed adjustments leads to the selection of an optimal configuration, fully aligned with ventilation standards for challenging environments, exemplified by underground basement car parks. This underscores not only the diagnostic power of CFD in pinpointing design inefficiencies but also its important role in providing actionable insights. These insights empower the MEP engineer to engineer solutions that not only meet but exceed regulatory ventilation standards in complex and confined spatial environments.

In summary, the examination of CFD applications for MEP systems underlines its vital role in addressing complex design challenges. Through real-world case studies, it appears that CFD is not just a tool but a highly effective method for achieving superior MEP system designs. The case studies, spanning a data center, a hospital operating room, and an underground car park, demonstrate CFD's precision and effectiveness in identifying deficiencies and optimizing critical parameters. In the healthcare sector, CFD serves as a crucial tool for ensuring compliance with codes and standards, with the potential to save lives by mitigating risks. The strategic application of CFD in the car park case study exemplifies its diagnostic power in pinpointing design inefficiencies and providing actionable insights, ultimately leading to optimal configurations that meet regulatory standards. Overall, CFD emerges as a transformative force in MEP engineering, offering not just accuracy but also invaluable insights for navigating the complexities of diverse and challenging environments.

However, the effective application of CFD demands a considerable level of expertise to accurately model complex systems and interpret simulation results. This expertise involves deep technical knowledge and substantial experience in the relevant field, along with proficiency in numerical data analysis. Experienced professionals are crucial for formulating accurate simulations that consider the complexities of real-world scenarios, accounting for numerous factors like instability, multiple phases, and sophisticated geometries. Their ability to interpret simulation outcomes, understand the implications of various parameters, and make informed decisions based on these results is important. Moreover, practical experience in using CFD tools and field-specific expertise enhance the accuracy and relevance of the simulations. Numerical data analysis skills play a crucial role in extracting meaningful insights from the vast amount of data generated during CFD simulations, enabling professionals to troubleshoot issues, optimize simulation setups, and draw valuable conclusions. In principle, the expertise required for successful CFD application involves a comprehensive skill set, consisting of theoretical understanding, practical experience, and analytical proficiency to ensure accurate and insightful simulation outcomes.

Acknowledgments

I would like to extend my sincere thanks and appreciation to all members of the Research and Development team at MEP Green Design and Build PLLC, with special recognition to Dustin Vu for his great help and support throughout the process of completing this paper. My gratitude also goes to Dr. Nan Muir, Osama Khayata, and Pat Powell for their critical reviews of the manuscript and their insightful recommendations.

References

1) Martin Liddament (1993) - A Review of Ventilation Efficiency.
2) ANSI/ASHRAE/ASHE Standard 170-2017 - Ventilation of Healthcare Facilities.
3) Texas Administrative Code (TAC), Title 25 – Health Services - Chapter 133
4) Hassan N. M. S., Khan* M. M. K., Rasul M. G. and MTO Amanullah (2012) - THERMAL PERFORMANCE MODELLING OF DATA CENTRE– A CASE STUDY
5) Stulz (2008) – Data Centre Cooling Best Practice